REFERENCE: **SAF/O3M/KNMI/VR/002**
ISSUE: 3/2014
DATE: 11 July 2014
PAGES: 55

O3M SAF VALIDATION REPORT

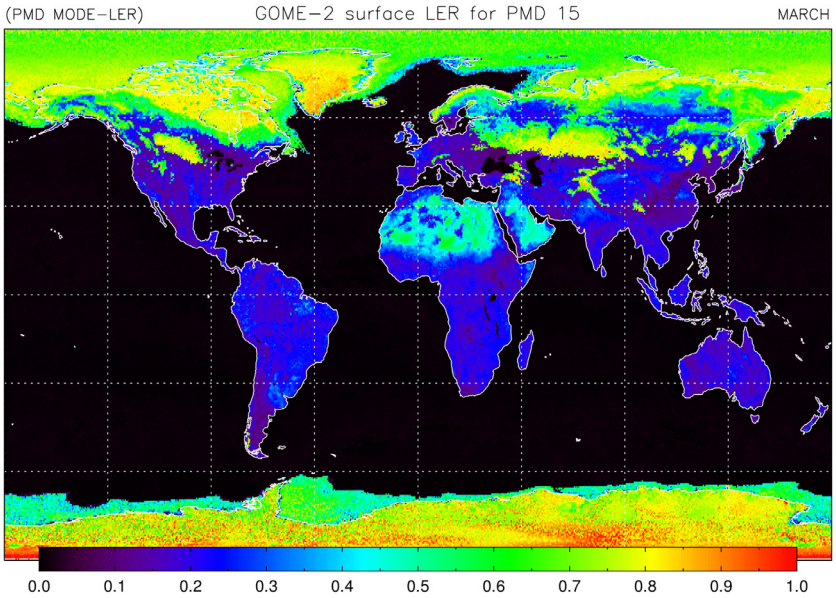

GOME-2 surface LER product

Product Identifier	Product Name
O3M-89	Surface LER from GOME-2 / MetOp-A

Authors	Institute
L.G. Tilstra	Royal Netherlands Meteorological Institute (KNMI)
O.N.E. Tuinder	Royal Netherlands Meteorological Institute (KNMI)
P. Stammes	Royal Netherlands Meteorological Institute (KNMI)

Document status sheet

Issue	Date	Page(s)	Modified Items / Reason for Change
1/2014	17-04-2014	all	first official version
2/2014	30-06-2014	all	changes and update after DRR
3/2014	11-07-2014	32,33	further changes after DRR

Contents

1 Introduction

1.1 Document purpose and scope

This document is the Validation Report (VR) for the GOME-2 surface LER products developed at KNMI in the framework of the O3M SAF (Satellite Application Facility on Ozone and Atmospheric Chemistry Monitoring). The aim of this VR is to present the validation approach, to present the results from the validation, and to report to the users the quality that they may expect.

1.2 GOME-2 surface LER products

The GOME-2 surface LER product contains two surface LER versions: one version based on GOME-2 observations by the Main Science Channels (MSCs) and one version based on GOME-2 observations by the Polarisation Measurement Devices (PMDs). The PMD-based version has the advantage over the MSC-based version that the surface LER is based on eight times as many observations, each with an eight times smaller footprint. This makes the retrieved surface LER less susceptible to residual cloud contamination, statistically more stable, and therefore more reliable. It also allows a higher spatial resolution of the end product, the surface LER database grid.

On the other hand, the surface LER of the PMD-based version is available only for a fixed list of wavelength bands. The exact wavelengths of the PMD bands are given in Table 3. This limitation is not an issue for the MSC-based surface LER. Here the wavelengths can be chosen freely (but within the continuum, avoiding absorption bands). The selected wavelength bands are given in Table 2.

1.3 Validation approach

Validation of the retrieved GOME-2 surface LER databases is performed by comparison with other surface LER databases that are discussed in section 2. From these, the GOME surface LER database [*Koelemeijer et al.*, 2003] makes most sense as a reference, because of the orbital and instrumental similarities between GOME and GOME-2, and their overlapping set of LER wavelength bands. Note that the GOME surface LER database was essentially retrieved using the MIN-LER approach (as explained in the ATBD), so a comparison with the GOME surface LER will in principle only allow validation of the GOME-2 surface LER determined using the MIN-LER approach.

The OMI surface LER database [*Kleipool et al.*, 2008] may be used for validation of the wavelengths below 500 nm. The OMI surface LER database is important as a reference because it uses the same surface LER retrieval approach as the one described in the ATBD. That is, both the GOME-2 MIN-

LER and the GOME-2 MODE-LER products can be compared to their OMI counterparts and this will provide information on the correctness of the GOME-2 surface LER algorithm and database.

Additionally, we compare the GOME-2 surface LER database with the MERIS black-sky albedo (BSA) database [*Popp et al.*, 2011]. This is strictly speaking not correct, because the BSA is the integral of the bidirectional reflectance distribution function (BRDF) over the entire hemisphere whereas the LER is derived from the much smaller range of viewing angles of the satellites observation geometry. Also, the LER approach by definition assumes a direction-independent surface albedo. Note that the comparison only makes sense over land, because the MERIS surface LER values over sea are not retrieved from MERIS observations. They were taken directly from the GOME surface LER database. As a result, the MERIS dataset only offers limited importance as a reference.

1.4 Suggested reading material

Herman, J. R., and E. A. Celarier (1997), Earth surface reflectivity climatology at 340–380 nm from TOMS data, *J. Geophys. Res., 102*(D23), 28,003–28,011, doi:10.1029/97JD02074 — HC1997

Koelemeijer, R. B. A., J. F. de Haan, and P. Stammes (2003), A database of spectral surface reflectivity in the range 335–772 nm derived from 5.5 years of GOME observations, *J. Geophys. Res., 108*(D2), 4070, doi:10.1029/2002JD002429 — KHS2003

Kleipool, Q. L., M. R. Dobber, J. F. de Haan, and P. F. Levelt (2008), Earth surface reflectance climatology from 3 years of OMI data, *J. Geophys. Res., 113*, D18308, doi:10.1029/2008JD010290 — KDHL2008

Popp, C., Wang, P., Brunner, D., Stammes, P., Zhou, Y., and Grzegorski, M. (2011), MERIS albedo climatology for FRESCO+ O2 A-band cloud retrieval, *Atmos. Meas. Tech., 4*, 463–483, doi:10.5194/amt-4-463-2011 — POPP2011

1.5 Abbreviations and acronyms

AAI	Absorbing Aerosol Index
ATBD	Algorithm Theoretical Basis Document
BRDF	Bidirectional Reflectance Distribution Function
BSA	Black-Sky Albedo
CDOP	Continuous Development & Operations Phase
DAK	Doubling-Adding KNMI
DU	Dobson Units, 2.69×10^{16} molecules cm^{-2}
EUMETSAT	European Organisation for the Exploitation of Meteorological Satellites

ENVISAT	Environmental Satellite
ERS	European Remote Sensing Satellite
ESA	European Space Agency
ETOPO-4	Topographic & Bathymetric data set from the NGDC, 4 arc-min. resolution
FOV	Field-of-View
FRESCO	Fast Retrieval Scheme for Cloud Observables
FWHM	Full Width at Half Maximum
GOME	Global Ozone Monitoring Experiment
HDF	Hierarchical Data Format
IT	Integration Time
KNMI	Koninklijk Nederlands Meteorologisch Instituut (De Bilt, NL)
LER	Lambert Equivalent Reflectivity
LUT	Look-Up Table
MERIS	Medium Resolution Imaging Spectrometer
MLS	Mid-Latitude Summer
MSC	Main Science Channel
NISE	Near-real-time Ice and Snow Extent
NOAA	National Oceanic and Atmospheric Administration
NGDC	NOAA's National Geophysical Data Center (Boulder, Colorado, USA)
NRT	Near-Real-Time
OMI	Ozone Monitoring Instrument
O3M SAF	Satellite Application Facility on Ozone and Atmospheric Chemistry Monitoring
PMD	Polarisation Measurement Device
PSD	Product Specification Document
PUM	Product User Manual
RTM	Radiative Transfer Model
SCIAMACHY	Scanning Imaging Absorption Spectrometer for Atmospheric Chartography
SZA	Solar Zenith Angle
TEMIS	Tropospheric Emission Monitoring Internet Service
TOA	Top-of-Atmosphere
TOMS	Total Ozone Mapping Spectrometer
UTC	Universal Time Co-ordinate
UV	Ultra-Violet
VIS	Visible
VZA	Viewing Zenith Angle

2 Surface reflectivity databases for the UV-VIS

2.1 Introduction

Surface reflectivity databases are needed for cloud, aerosol and trace gas retrievals. One of the first surface reflectivity databases retrieved using UV satellite remote sensing techniques is the Total Ozone Mapping Spectrometer (TOMS) [*Heath et al.*, 1975] surface LER database [*Herman and Celarier*, 1997]. The retrieved reflectivity is the Lambert equivalent reflectivity (LER) of the surface found from scenes which are assumed to be cloud free. The retrieval method relies on the removal of the (modelled) atmospheric contribution from the (observed) top-of-atmosphere (TOA) reflectance. In this approach the surface is defined to behave as a Lambertian reflector. The TOMS surface LER database ($1.25^\circ \times 1^\circ$) was retrieved for 340 and 380 nm only, which limits its usefulness.

The GOME [*Burrows et al.*, 1999] surface reflectivity database provides the surface LER on a $1^\circ \times 1^\circ$ grid for 11 wavelength bands between 335 and 772 nm [*Koelemeijer et al.*, 2003]. Although this is already quite an improvement with respect to the TOMS surface LER database, the database is still limited in quality by the low number of measurements from which the surface LER had to be extracted and the large GOME footprint size (see Table 1). In particular, pixels over sea are often affected by residual cloud contamination. In these cases the surface LER was retrieved from scenes which were not sufficiently cloud free. In other cases, e.g. snow surfaces, the surface LER was retrieved from a few measurements which were not representative for the entire month.

A large improvement on these points is the OMI surface reflectivity database [*Kleipool et al.*, 2008]. First, the OMI instrument [*Levelt et al.*, 2006] has a much smaller footprint size (24×13 km^2 at nadir) combined with a larger global coverage (see Table 1). This leads to better statistics and results in a higher accuracy for the surface LER retrieval. Second, the higher number of measurements allows for inspecting the distribution of scene LERs for each grid cell, and for making a more sophisticated selection of representative (cloud-free) scenes instead of directly taking the minimum scene LER value like in the case of the TOMS and GOME databases. Third, the provided OMI surface LER database has a higher spatial resolution ($0.5^\circ \times 0.5^\circ$ grid). The limiting factor is the OMI wavelength range. The longest wavelength in the OMI surface LER database is 499 nm.

The GOME-2 series of satellite instruments does not have the limitations of the above instruments and therefore can be used to create a better surface LER database. It has the spectral range of GOME but a much smaller footprint (80×40 km^2) which is constant over the full swath width. The number of measurements that are available per longitude/latitude cell in the database grid is smaller than that of OMI, but enough to perform a statistical analysis on the distribution of retrieved scene LERs. In the ATBD the approach that was used for the OMI surface reflectivity database is followed closely.

The main advantage of the GOME-2 surface LER database with respect to the OMI surface LER database is the wider wavelength range of the GOME-2 instrument. Additionally, the retrieval algorithm uses aerosol information, available via the GOME-2 Absorbing Aerosol Index (AAI) product, to filter out scenes with large aerosol loadings, as these scenes can result in inaccurate values of the retrieved surface LER. This filtering is especially important for locations over desert areas.

2.2 Tables

In Table 1 we summarise the properties of the discussed surface reflectivity databases. For GOME-2 we provide the specifications for the MSC-based and PMD-based algorithms. In Table 2 we list the wavelength bands of the surface reflectivity databases, and their application. In Table 3 we provide the wavelengths of the GOME-2 PMD bands, relevant to the PMD-based algorithm. The selection of the wavelength bands for the GOME-2 MSC-LER was influenced largely by the already existing surface LER databases. Below 325 nm the surface contribution to the TOA reflectance is low, which prevents an accurate retrieval of the surface LER below this wavelength. For the GOME-2 PMD-LER this means that the surface LER for PMD 1 and 2 cannot be retrieved, as indicated.

instrument	TOMS	GOME	OMI	MSC - GOME-2 - PMD	
satellite	Nimbus-7	ERS-2	Aura	MetOp-A/B	
equator crossing time (LT)	12:00	10:30	13:45	09:30	
dayside flight direction	S→N	N→S	S→N	N→S	
number of days for global coverage	1	3	1	1.5	
pixel size at nadir (km × km)	50 × 50	320 × 40	24 × 13	80 × 40	10 × 40
number of usable pixels per orbit	∼12000	∼1300	∼83000	∼11000	∼88000
dataset time range (*)	1978–1993	1995–2000	2005–2009	2007→ (*)	2008→ (*)
selected wavelength bands	2	11	23	15	13
wavelength range covered	340–380	335–772	328–499	325–772	325–799
band width (nm)	1.0	1.0	1.0	1.0	see text
spatial resolution (°lon × °lat)	1.25 × 1.0	1.0 × 1.0	0.5 × 0.5	1.0 × 1.0	0.5 × 0.5
reference	HC1997	KHS2003	KDHL2008	this work	

Table 1: Characteristics and properties of the UV-VIS surface LER databases, and of the satellite instruments from which they are derived. Wavelength band information can be found in Tables 2/3.

(*)The longer the time period covered, the higher the number of times a certain region has been observed. This increases the chances of having observed this region under clear sky conditions. Occasional reprocessing over longer time periods therefore increases the quality, stability, and reliability of the surface LER product. GOME-2 data are available from January 2007 (MetOp-A). GOME-2 data from MetOp-B are available since December 2012.

λ (nm)	TOMS	GOME	OMI	GOME-2	application / relevance
325				+	LER, ozone, HCHO, SO_2
328			+		LER, ozone, HCHO
335		+	+	+	LER, ozone, HCHO
340	+			+	LER, aerosol, HCHO, BrO
342			+		LER, aerosol, HCHO, BrO
345			+		LER, aerosol, HCHO, BrO
354			+	+	LER, aerosol, HCHO, BrO, OClO
367			+		LER, aerosol, OClO
372			+		LER, aerosol, OClO
376			+		LER, aerosol, OClO
380	+	+	+	+	LER, aerosol, OClO
388			+	+	LER, aerosol, OClO
406			+		LER, aerosol
416		+	+	+	LER, aerosol
418			+		LER, aerosol
425			+		LER, aerosol, NO_2
440		+	+	+	LER, aerosol, NO_2
442			+		LER, aerosol, NO_2
452			+		LER, aerosol, NO_2
463		+	+	+	LER, aerosol, NO_2, O_2-O_2
471			+		LER, aerosol, NO_2, O_2-O_2
477			+		LER, aerosol, NO_2, O_2-O_2
488			+		LER, aerosol, NO_2, O_2-O_2
494		+	+	+	LER, aerosol, NO_2
499			+		LER, aerosol
555		+		+	LER, aerosol
610		+		+	LER, aerosol, H_2O
670		+		+	LER, aerosol, H_2O, O_2-B
758		+		+	LER, aerosol, O_2-A
772		+		+	LER, aerosol, O_2-A
Total:	2	11	23	15	

Table 2: Wavelength bands of the four monochromatic surface LER databases, and their applications. All wavelength bands are located outside strong gaseous absorption bands in order to avoid complicated modelling of the radiative transfer. The number of wavelength bands is also given.

PMD	λ (nm)	application / relevance	PMD	λ (nm)	application / relevance
01	312	not retrieved	09	460	LER, aerosol, NO_2, O_2-O_2
02	317	not retrieved	10	519	LER, aerosol
03	325	LER, ozone, HCHO, SO_2	11	554	LER, aerosol
04	332	LER, ozone, HCHO	12	589	LER, aerosol
05	338	LER, aerosol, HCHO, BrO	13	639	LER, aerosol, H_2O
06	369	LER, aerosol, OClO	14	756	affected by O_2 absorption
07	382	LER, aerosol, OClO	15	799	LER, aerosol
08	413	LER, aerosol			

Table 3: Wavelength information for the PMD bands used in the PMD-based surface LER algorithm. The wavelength definition follows PMD band definition v3.1, so the list applies to MetOp-A PMD data from after 11 March 2008 as well as to all MetOp-B PMD data.

The widths of the PMD bands are not provided in Table 3, but these (and other information) can be found in the "GOME-2 Factsheet" [*EUMETSAT*, 2014]. For some of the PMD bands the relatively broad wavelength range covered leads to inference with absorption bands. For instance, PMD 14 overlaps with the oxygen-A absorption band and this has affected the retrieved surface LER.

3 MSC-LER: Comparison with GOME-1

In this section, we compare the GOME-2 surface LER product with the GOME-1 surface LER product. Because of the orbital and instrumental similarities between GOME-1 and GOME-2, the GOME-1 surface LER product should, at least on paper, be the ideal reference. Note, however, that the GOME-1 surface LER database was retrieved using the MIN-LER approach (as explained in the ATBD). As a result, the GOME-1 surface LER database can only be used to validate the GOME-2 surface LER database determined using the MIN-LER approach.

All eleven wavelength bands of the GOME-1 surface LER database were included in the GOME-2 surface LER database. We can, therefore, analyse the entire wavelength range covered.

3.1 Global maps of the differences

For each month of the year and for each wavelength band in the GOME-1 surface LER database (see Table 2) we calculate the difference in surface LER provided by the GOME-2 and GOME-1 surface LER databases. A typical outcome is shown in Figure 1, which presents a global map of the surface LER difference at the 772-nm wavelength band for the month March. The overall quality is good, but the GOME-2 surface LER is lower than the GOME-1 surface LER. The difference is clearly dependent on surface type. For surfaces with a higher surface reflectivity (land, snow, ice surfaces) the bias is more negative than for surfaces with a lower surface reflectivity (ocean surfaces).

There are a few regions where the surface LER difference is found to be positive (indicated by the red areas in Figure 1). At a first glance, some of these red areas appear to be partly caused by differences in snow/ice presence. Such differences could in principle be related to actual differences in the snow/ice situation during the observed periods (GOME-1: 1995–2000; GOME-2: 2007–2013). Note, however, that some of the "red" regions are located close to land/sea boundaries. This is rather suspicious and the large pixel size of the GOME-1 measurements (see Table 1) may have had a hand in the appearance of these features. Also notice that the correction for cloud contamination in the GOME-1 surface LER retrieval produces certain features in Figure 1. To be more explicit, as an example the $5^\circ \times 5^\circ$ box near 80°N, 0°E coincides with one of the $5^\circ \times 5^\circ$ boxes used in the algorithm to search for replacement values [*Koelemeijer et al.*, 2003].

In Figure 2 we present a similar plot for the same month of the year (March) but for the 494-nm wavelength band. For this wavelength band the agreement between the GOME-2 and GOME-1 surface LER appears to be better. Over the ocean the absolute difference is lower than at 772 nm and well within the 0.01 level, despite the fact that the surface LER at 494 nm is normally larger than at 772 nm (and larger differences could be expected). The remaining larger negative values can

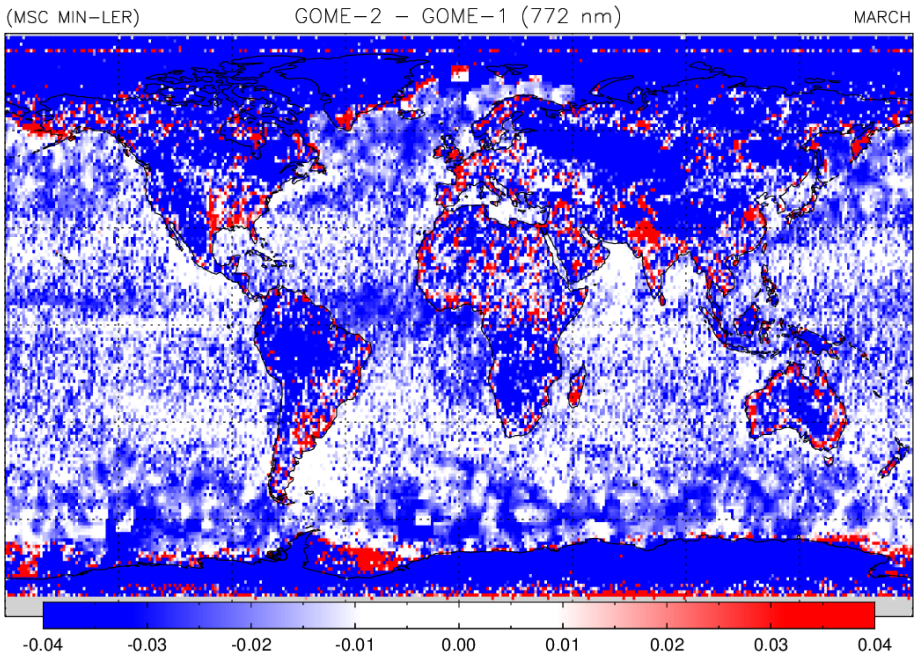

Figure 1: Map of the difference between the 772-nm surface LER from the GOME-2 and GOME-1 surface LER databases. The MIN-LER is used here. Over the ocean, the agreement is fair, but there clearly is a negative offset. Over land, this negative bias can go up to as much as 0.04.

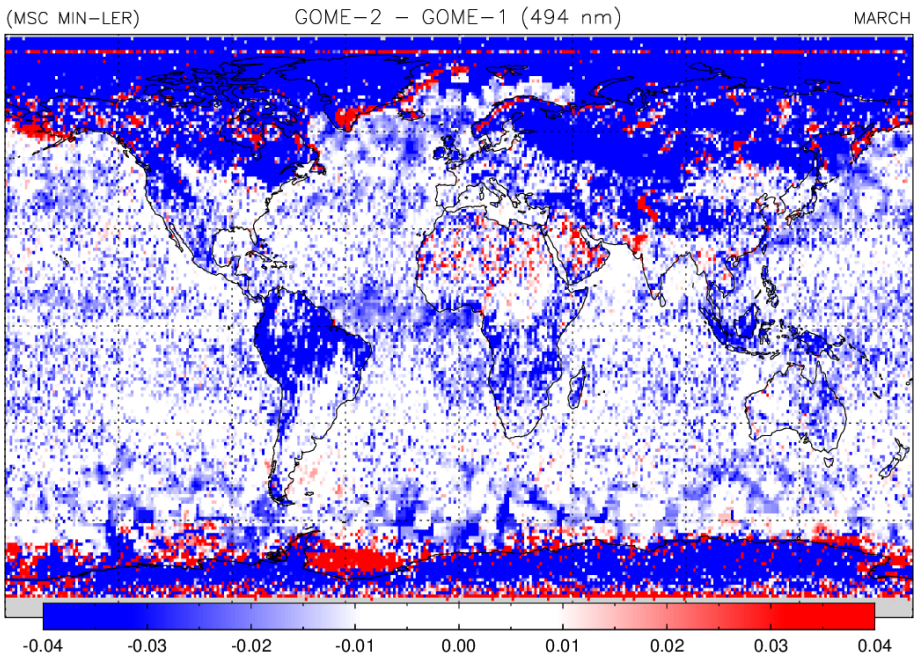

Figure 2: Map of the difference between the 494-nm surface LER from the GOME-2 and GOME-1 surface LER databases. Over the ocean, the agreement is good, but also for this wavelength there is an offset. Over land, the agreement is good, apart from a negative bias.

be related to remaining cloud contamination in the GOME-1 surface LER. Over land the negative bias found earlier at 772 nm is again present, albeit less pronounced than for the 772-nm wavelength band. The agreement seems to be better at 494 nm compared to 772 nm, but this may also be caused by the fact that the surface LER values over land are also typically lower at 494 nm than at 772 nm. For snow/ice surfaces the negative bias is maximal, which again points to a dependence of the surface LER difference on surface type. All in all the agreement is good also for this wavelength band.

3.2 Statistical analysis of the differences

To provide a more statistical analysis of the differences between the GOME-2 and GOME-1 surface LER databases, we present in Figure 3 histograms of the surface LER differences. We only consider surface LER data with latitudes between 60°N and 60°S, thereby excluding data measured for extreme solar zenith angles as well as data located near the polar regions. The histograms are provided for each month of the year, for the 494-nm wavelength band. The mean of the distribution is represented by the dashed vertical line, the mode of the distribution is given by the dotted vertical line. The histograms in Figure 3 confirm the lower values already reported in the previous section.

In Figure 4 we present the result for the same month for the 772-nm wavelength band. The results are different in the sense that the distributions are somewhat asymmetric. This may be a result of the correction for cloud contamination in the GOME-1 surface LER retrieval. This correction basically copies the surface LER from potentially a single "clear-sky" ocean grid cell to many "cloud contaminated" ocean grid cells. This procedure can alter the shape of the distribution considerably. In any case, the result confirms the lower values for the GOME-2 surface LER reported earlier.

To provide more quantitative information, we tabulate in Table 4 the results for all months and all wavelengths. Looking at the data we see that the mean difference is only slightly dependent on the month of the year. No clear seasonal variation can be extracted. The same can be said about the spread (FWHM) of the distribution: it does not depend much on the month of the year.

Note that the wavelength bands at 335 and 380 nm seem to be showing slightly different behaviour than the other wavelength bands. For instance, the bias is positive for 380 nm, where it is negative for all the others wavelength bands. The spread (FWHM) of the distribution is larger for the 335 and 380 nm wavelength bands than for the others. An explanation for the bias is the impact of instrument degradation on the GOME-1 surface LER database, as reported by *Koelemeijer et al.* [2003]. This has for sure had an impact on the 335 and 380 nm results. It does not, however, explain the increase in the spread of the distribution. The increase of the spread of the distribution is presumably a result of the increased difficulty of observing the surface at the shorter wavelengths.

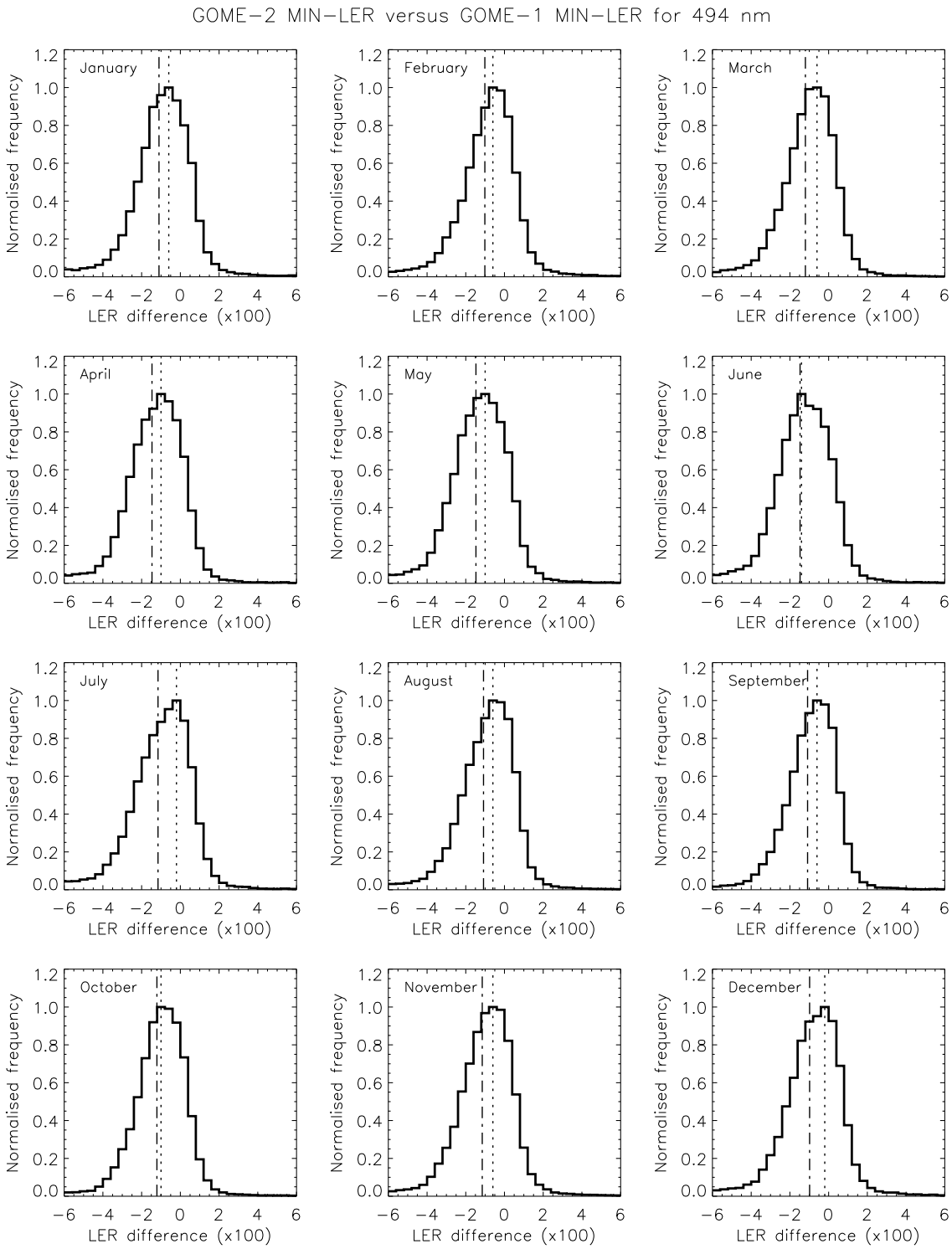

Figure 3: Histogram of the differences in the surface LER databases of GOME-2 and GOME-1 at 494 nm. The GOME-1 surface LER database was determined according to the MIN-LER approach, which means that we can only validate the GOME-2 MIN-LER product. The vertical lines indicate the mean (dashed line) and the mode (dotted line) of the distribution.

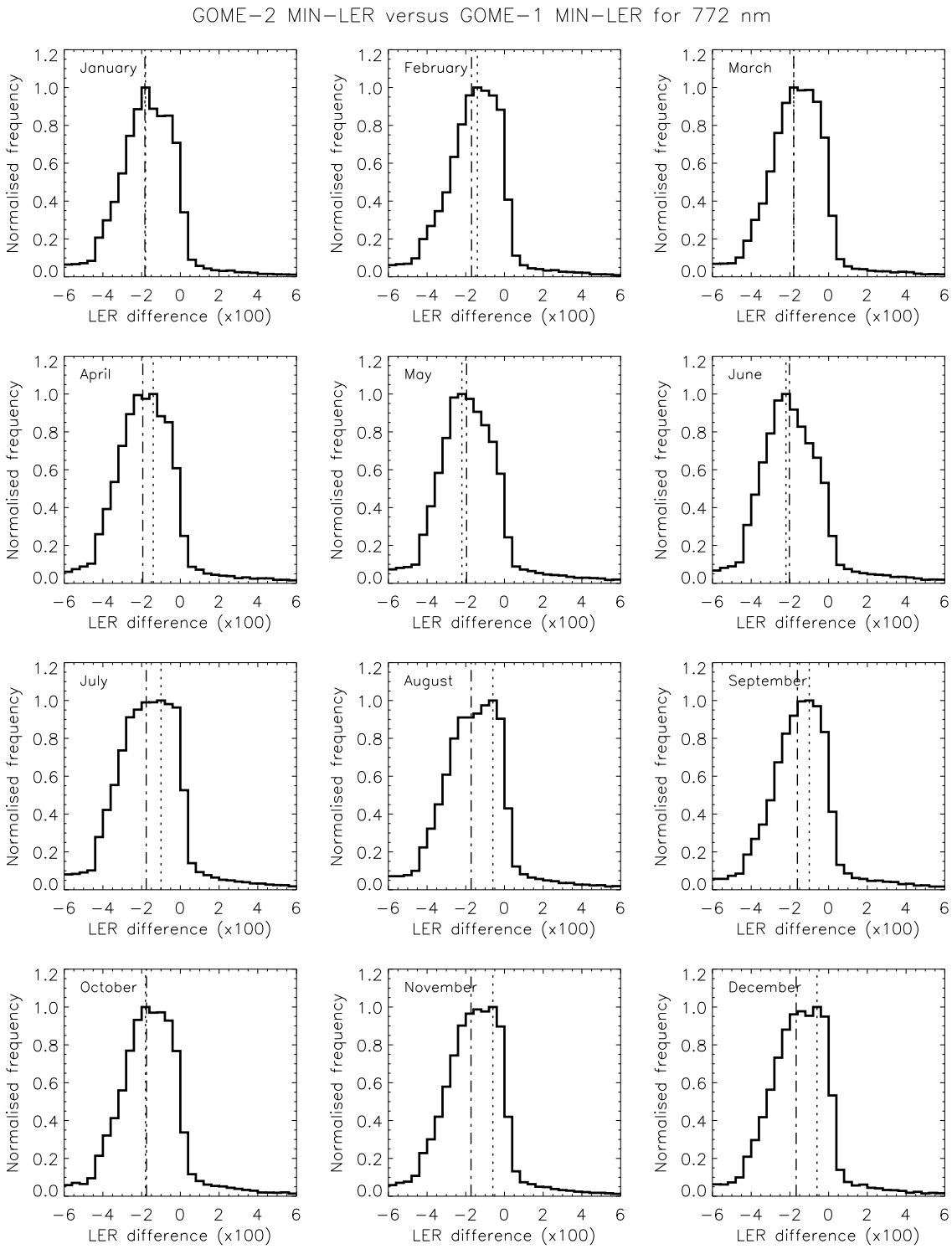

Figure 4: Histogram of the differences in the surface LER databases of GOME-2 and GOME-1 at 772 nm. For this wavelength the histograms are somewhat asymmetric. This might be related to the correction for cloud contamination over the ocean (either for GOME-1, GOME-2, or both). The vertical lines indicate the mean (dashed line) and the mode (dotted line) of the distribution.

GOME-2 versus GOME-1 (MIN-LER)												
Mean surface LER difference ($\times$100)												
λ (nm)	JAN	FEB	MAR	APR	MAY	JUN	JUL	AUG	SEP	OCT	NOV	DEC
335	-0.17	-0.09	0.02	-0.60	-0.84	-1.24	-0.22	-0.28	-0.31	-0.44	-0.52	-0.23
380	0.50	0.66	0.63	0.30	0.15	0.01	0.52	0.66	0.69	0.49	0.44	0.54
416	-0.45	-0.43	-0.59	-0.97	-0.97	-1.03	-0.71	-0.66	-0.55	-0.63	-0.67	-0.40
440	-0.91	-0.80	-0.96	-1.28	-1.27	-1.33	-1.00	-0.96	-0.87	-0.97	-1.00	-0.77
463	-1.03	-0.91	-1.10	-1.37	-1.40	-1.42	-1.08	-1.04	-0.96	-1.07	-1.06	-0.89
494	-1.10	-1.01	-1.20	-1.46	-1.47	-1.47	-1.15	-1.08	-1.09	-1.21	-1.15	-0.98
555	-1.44	-1.30	-1.47	-1.69	-1.74	-1.82	-1.42	-1.34	-1.30	-1.43	-1.39	-1.28
610	-1.54	-1.42	-1.58	-1.73	-1.75	-1.82	-1.44	-1.42	-1.42	-1.55	-1.48	-1.38
670	-1.70	-1.57	-1.73	-1.93	-1.94	-2.02	-1.62	-1.60	-1.59	-1.74	-1.65	-1.54
758	-1.81	-1.68	-1.79	-1.93	-1.96	-1.99	-1.76	-1.69	-1.60	-1.74	-1.72	-1.64
772	-1.83	-1.70	-1.80	-1.94	-1.96	-2.03	-1.76	-1.72	-1.61	-1.75	-1.73	-1.67
FWHM of distribution ($\times$100)												
λ (nm)	JAN	FEB	MAR	APR	MAY	JUN	JUL	AUG	SEP	OCT	NOV	DEC
335	4.24	4.30	4.40	4.37	4.77	4.98	4.84	5.20	4.99	4.75	4.87	4.87
380	3.27	3.24	3.29	3.49	3.62	3.64	3.68	3.41	3.22	3.22	3.35	3.45
416	3.19	3.11	3.08	3.25	3.33	3.35	3.31	3.13	3.00	3.03	3.17	3.19
440	3.12	3.00	2.97	3.17	3.30	3.31	3.27	3.05	2.90	2.92	3.07	3.11
463	2.99	2.83	2.82	3.08	3.18	3.22	3.16	2.95	2.75	2.77	2.95	2.99
494	2.87	2.72	2.74	3.06	3.17	3.14	3.16	2.89	2.70	2.72	2.89	2.93
555	2.96	2.79	2.81	3.06	3.14	3.28	3.27	2.97	2.80	2.85	3.00	3.03
610	2.98	2.82	2.83	3.00	3.08	3.20	3.21	2.89	2.77	2.86	3.03	3.05
670	2.98	2.84	2.86	3.08	3.12	3.23	3.27	2.99	2.81	2.92	3.06	3.05
758	3.10	2.95	3.00	3.24	3.30	3.39	3.57	3.35	3.03	3.10	3.20	3.21
772	3.14	2.99	3.03	3.22	3.25	3.36	3.53	3.33	3.05	3.14	3.22	3.26

Table 4: Mean difference in the surface LER of the GOME-2 and GOME-1 surface LER databases. The FWHM of the distribution is also given. The numbers have been multiplied by 100.

3.3 Conclusion of the comparison with GOME-1

The main result of the analysis is that the agreement between the GOME-2 and GOME-1 surface LER databases is in principle quite good, but that the GOME-2 surface LER values are in general lower (up to 0.04 in magnitude) than the GOME-1 surface LER values. The magnitude of the difference seems to be dependent on the surface type (and on the surface LER). This could point to differences due to differences in the radiometric calibration of the instruments. Despite this, the magnitude of the reported bias is relatively small, and the agreement is in general good.

4 MSC-LER: Comparison with OMI

In this section, we compare the GOME-2 surface LER product with the OMI surface LER product. The orbital parameters for GOME-2 and OMI are quite different (see Table 1) which makes the comparison less than ideal from this point of view. On the other hand, we can perform the comparison for both the MIN-LER and the MODE-LER products because the OMI surface LER product contains both of these surface LER types. Unfortunately, because of the limited wavelength range of OMI, only the eight wavelength bands from 335 to 494 nm can be compared in this study.

4.1 Global maps of the differences

In Figure 5 we present the difference between the 494-nm surface LER for the month March from the GOME-2 MIN-LER and OMI MIN-LER databases. The agreement is in general rather good. Over the ocean the differences are very close to zero. For some areas over the ocean there a slightly negative differences. One explanation could be different performance of the correction for cloud contamination for the OMI surface LER over the ocean. The differences are in any case very small. Over land the differences are close to zero for most non-snow/ice surfaces. We find negative values (for parts of Australia, South America, and the African continent) but also positive values (for parts of Asia and desert areas like the Sahara). The differences are, in general, to be considered small.

Larger differences are found for the snow/ice covered surfaces. In fact, for most of the snow/ice related surfaces the GOME-2 surface LER is smaller by values approaching -0.04 compared to the OMI surface LER. For some areas, the differences are positive, reaching values of 0.04. This behaviour is clearly related to the snow/ice situation in the scene. As the MIN-LER is based on the minimum LER found in the time period used, changes in the actual snow/ice situation will have a large impact. For that reason, the switching from blue to red seems to be correct behaviour, considering the differences in the time period covered. But, there appears to be a negative bias for the snow/ice surfaces. This bias could be the result of the different overpass times, or different observation geometries (BRDF), but it could also be the result of differences in the radiometric calibration of the two instruments.

In Figure 6 we present the global map of the differences between the MODE-LER of GOME-2 and OMI, again for the month March. The plot is comparable to the one in Figure 5. A red-coloured feature is present in Northern Africa, close to the equator. This feature is caused by the fact that the switch from 1% accumulated value to the mode of the scene LER distribution takes place at a different location. This is the result of a difference between the two algorithms. The OMI surface LER retrieval uses the FWHM of the scene LER distribution to determine whether or not the mode should be used. The GOME-2 surface LER retrieval on the other hand uses the standard deviation of the scene LER distribution. In general, the MODE-LER over land is a bit more negative than the

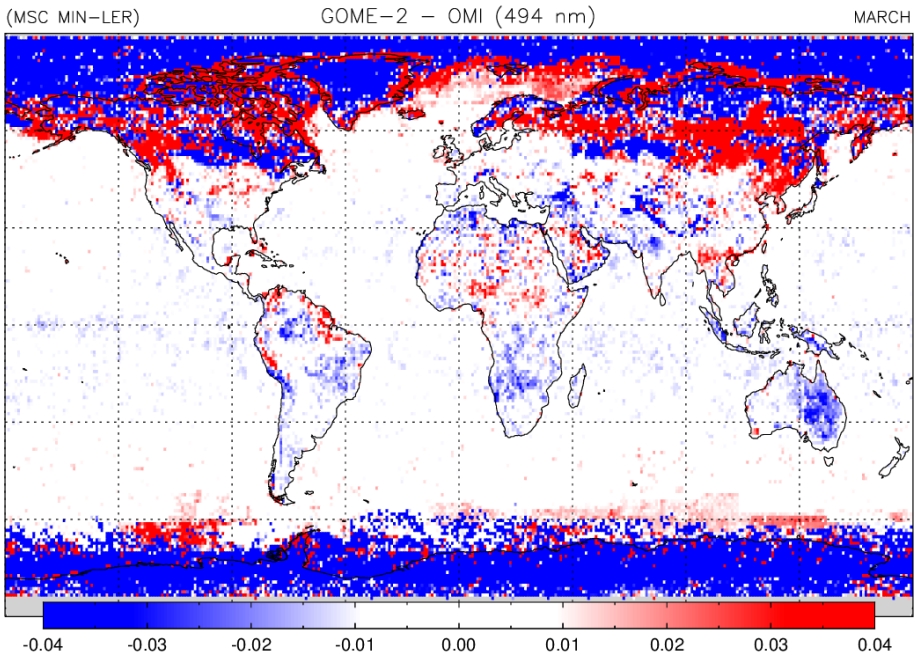

Figure 5: Map of the difference between the 494-nm surface LER from the GOME-2 and OMI MIN-LER databases, for the month March. Over the ocean, the agreement is good with deviations generally far below the 0.01 level. Above snow/ice areas, the deviations are systematically larger.

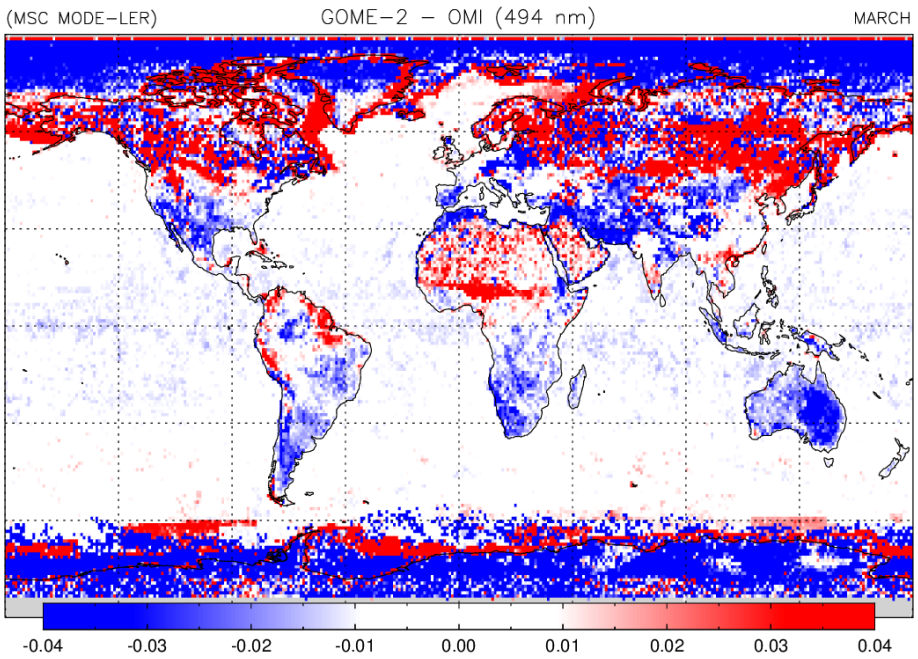

Figure 6: Map of the difference between the 494-nm surface LER from the GOME-2 and OMI MODE-LER databases, for the month March. Over the ocean, the agreement is good. Above land, the agreement is generally good, apart from differences related to snow/ice cover and extent.

MIN-LER. For the snow/ice surfaces near the North and South pole, there appears to be a bit more "white" in the MODE-LER difference as compared to the MIN-LER difference.

4.2 Statistical analysis of the differences

We calculate the distributions of the differences for each month of the year, for each of the OMI surface LER wavelength bands that coincide with the GOME-2 surface LER wavelength bands (see Table 2). This is done for the MIN-LER and MODE-LER surface LER products.

4.2.1 MIN-LER product

In Figure 7 we present the results for the MIN-LER product. The histograms are histograms of the distribution of the differences between GOME-2 and OMI for 380 nm. As can be seen, the histograms are symmetric and have their mean and mode values close to zero. The bias is only slightly higher than zero, on the order of 0.01. This is the case for all months of the year. In Figure 8 we present the same result, but then for the 494 nm wavelength band. The bias is negative, but negligible. The width of the distribution is smaller than at 380 nm. This is to be expected because the majority of the grid cells are located over the ocean and for these cases the surface LER itself is smaller at 494 nm than at 380 nm. All in all the agreement is found to be very good.

In Table 5 we present the numerical results of the histogram analyses. The table presents the mean surface MIN-LER difference for each month of the year and for each of the eight wavelength bands that could be compared. It also lists the spread (FWHM) of the distribution. All numbers were multiplied by 100. Note that especially for the wavelength bands of 388 nm and above the agreement is very good. Also notice that the spread of the difference distribution is much smaller than that found for the GOME-1 versus GOME-2 comparison (as reported in Table 4).

4.2.2 MODE-LER product

In Figures 9 and 10 and we again present plots of the histograms of the differences for the 380 and 494 nm wavelength bands, but this time for the MODE-LER. From the 380-nm result we conclude that the results are comparable to the MIN-LER result shown before in Figure 7. The shape of the distribution is similar, and the mean and mode of the distributions are close to zero. Also for the 494-nm result the distributions are very similar to the MIN-LER result shown before in Figure 8.

In Table 6 we present, in the usual manner, the numerical results of the comparison. Comparing with the results presented earlier in Table 5 we see that the values are very comparable. This is especially

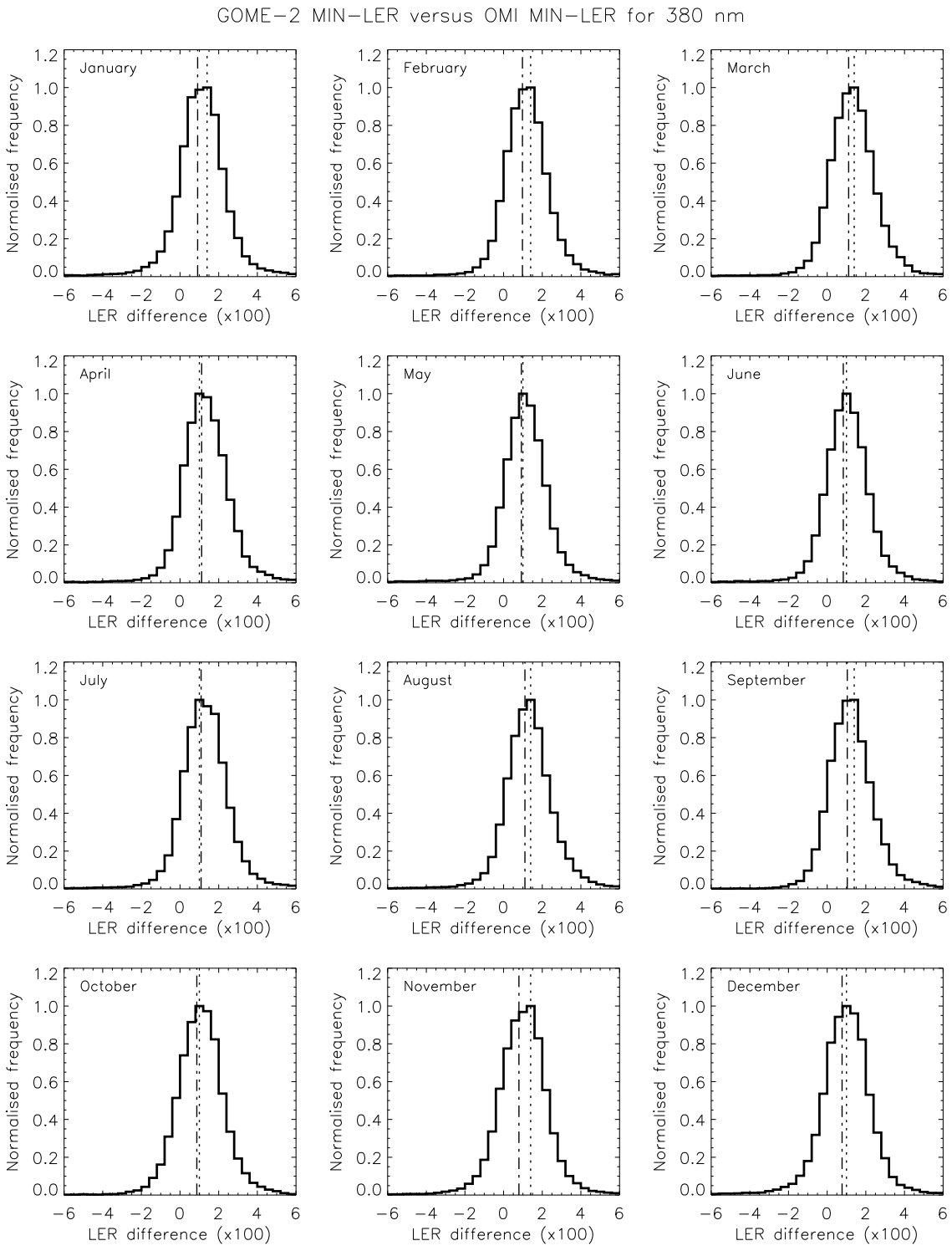

Figure 7: Histogram of the differences in the surface LER databases of GOME-2 and OMI at 380 nm. The MIN-LER products are compared. There seems to be a small systematic offset. The vertical lines indicate the mean (dashed line) and the mode (dotted line) of the distribution.

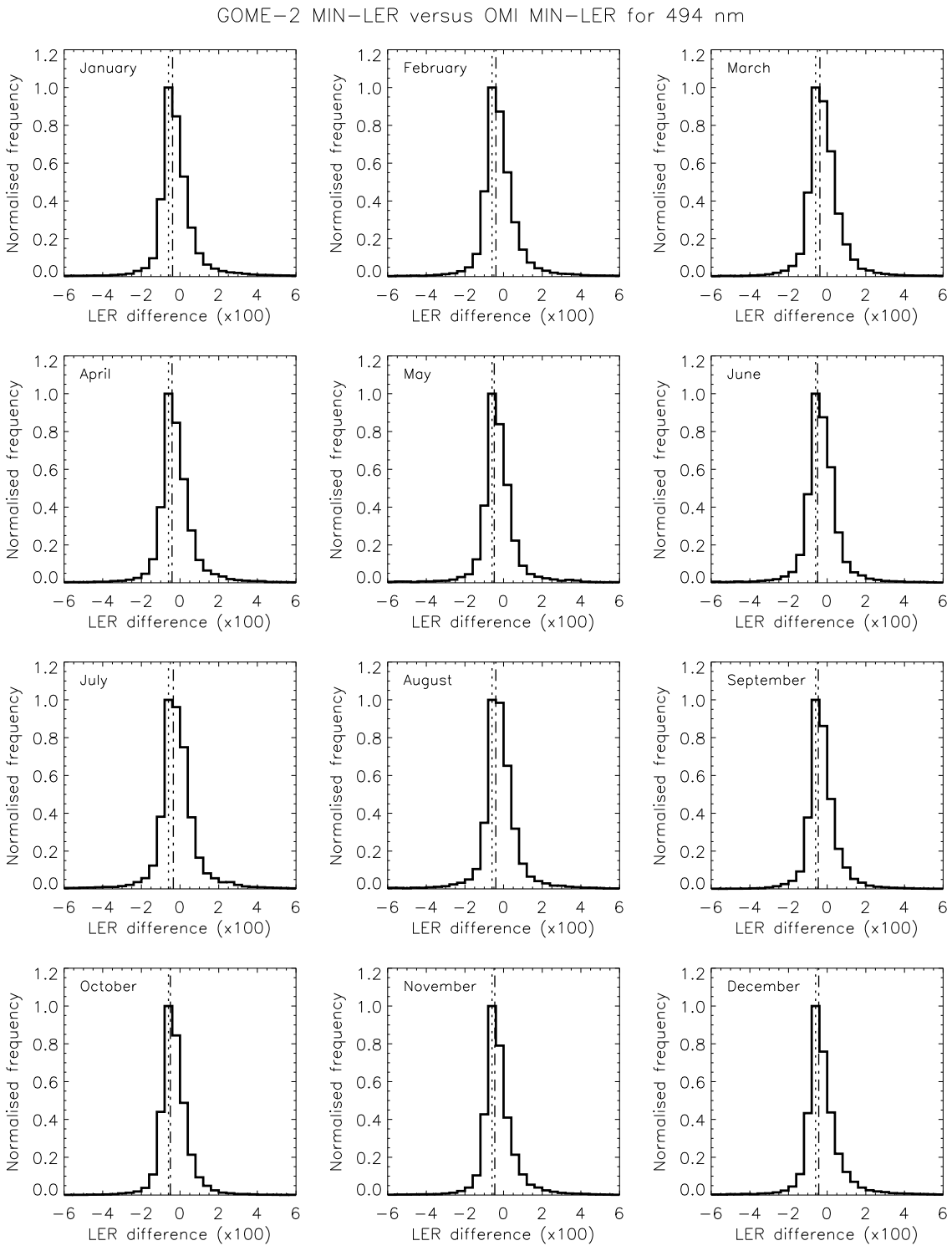

Figure 8: Histogram of the differences in the surface LER databases of GOME-2 and OMI at 494 nm. The MIN-LER products are compared. The agreement is very good for all the months. The vertical lines indicate the the mean (dashed line) and the mode (dotted line) of the distribution.

GOME-2 versus OMI (MIN-LER)												
Mean surface LER difference ($\times$100)												
λ (nm)	JAN	FEB	MAR	APR	MAY	JUN	JUL	AUG	SEP	OCT	NOV	DEC
335	1.96	1.95	1.94	1.74	1.29	1.09	1.53	1.75	1.86	1.83	1.77	1.77
354	1.17	1.22	1.31	1.21	0.88	0.73	1.06	1.18	1.24	1.16	1.10	1.04
380	0.91	0.97	1.11	1.12	0.92	0.83	1.09	1.10	1.04	0.87	0.79	0.77
388	0.45	0.55	0.69	0.72	0.55	0.47	0.68	0.70	0.62	0.44	0.35	0.32
416	-0.00	-0.01	0.03	-0.02	-0.19	-0.25	-0.05	-0.02	-0.02	-0.05	-0.05	-0.06
440	-0.31	-0.31	-0.28	-0.31	-0.45	-0.50	-0.28	-0.31	-0.34	-0.40	-0.39	-0.37
463	-0.39	-0.39	-0.36	-0.39	-0.50	-0.52	-0.34	-0.39	-0.43	-0.49	-0.46	-0.43
494	-0.39	-0.40	-0.37	-0.41	-0.48	-0.49	-0.35	-0.40	-0.46	-0.50	-0.46	-0.44
FWHM of distribution ($\times$100)												
λ (nm)	JAN	FEB	MAR	APR	MAY	JUN	JUL	AUG	SEP	OCT	NOV	DEC
335	2.49	2.38	2.34	2.31	2.36	2.49	2.50	2.47	2.38	2.49	2.58	2.61
354	2.27	2.20	2.21	2.13	2.20	2.32	2.31	2.24	2.27	2.35	2.44	2.45
380	2.42	2.34	2.49	2.46	2.28	2.33	2.46	2.43	2.42	2.54	2.59	2.56
388	2.34	2.24	2.38	2.38	2.18	2.22	2.35	2.28	2.31	2.43	2.51	2.46
416	1.90	1.91	2.03	1.92	1.83	1.81	1.84	1.83	1.75	1.87	1.95	1.98
440	1.68	1.71	1.79	1.71	1.58	1.68	1.75	1.67	1.57	1.62	1.65	1.73
463	1.46	1.50	1.58	1.52	1.44	1.51	1.60	1.46	1.37	1.44	1.43	1.47
494	1.25	1.32	1.39	1.29	1.23	1.34	1.40	1.27	1.15	1.20	1.15	1.21

Table 5: Mean difference in the surface LER of the GOME-2 and OMI surface LER databases. The FWHM of the distribution is also given. The numbers have been multiplied by 100.

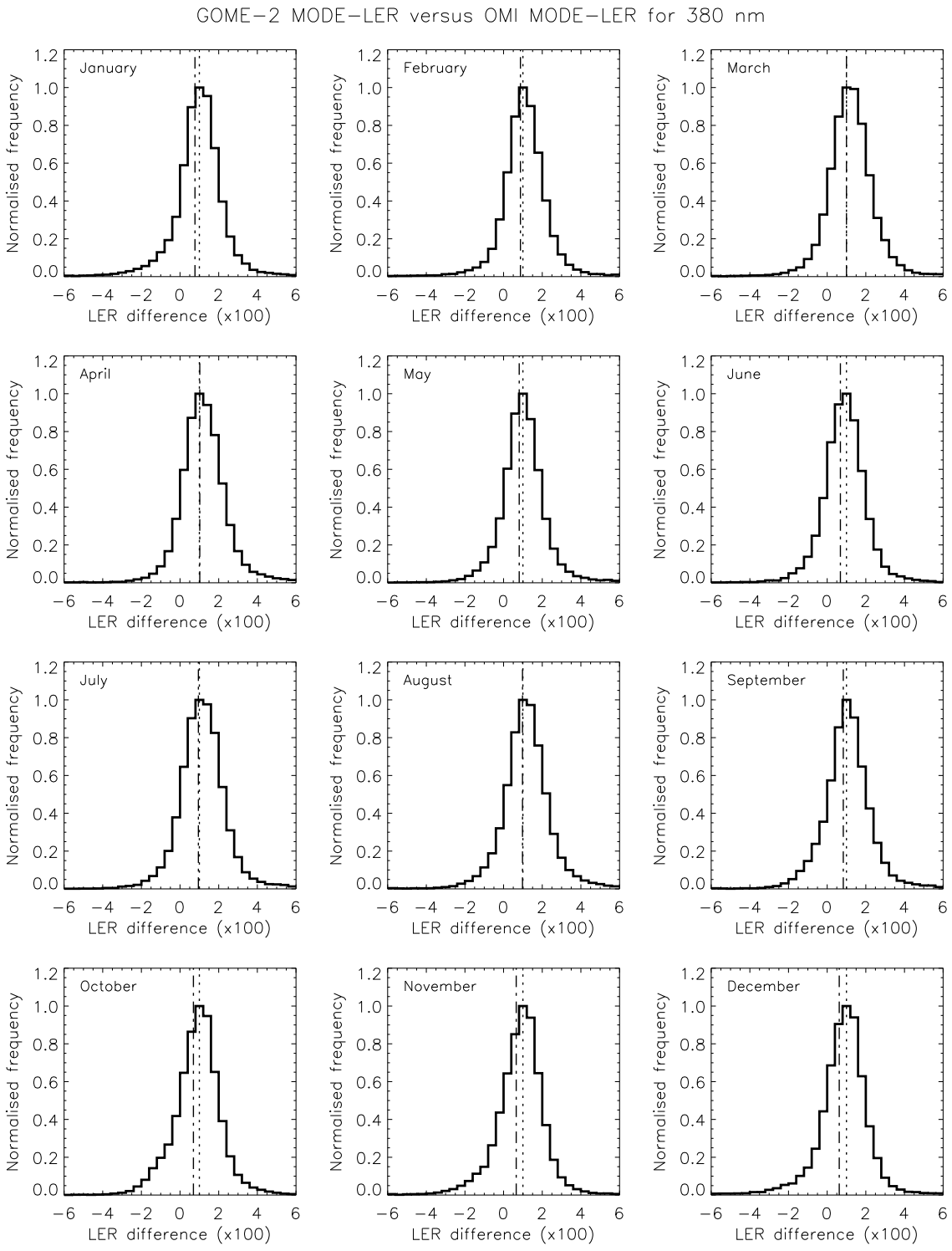

Figure 9: Histogram of the differences in the surface LER databases of GOME-2 and OMI at 380 nm. This time the MODE-LER products are compared. The agreement is good for all the months. The vertical lines indicate the mean (dashed line) and the mode (dotted line) of the distribution.

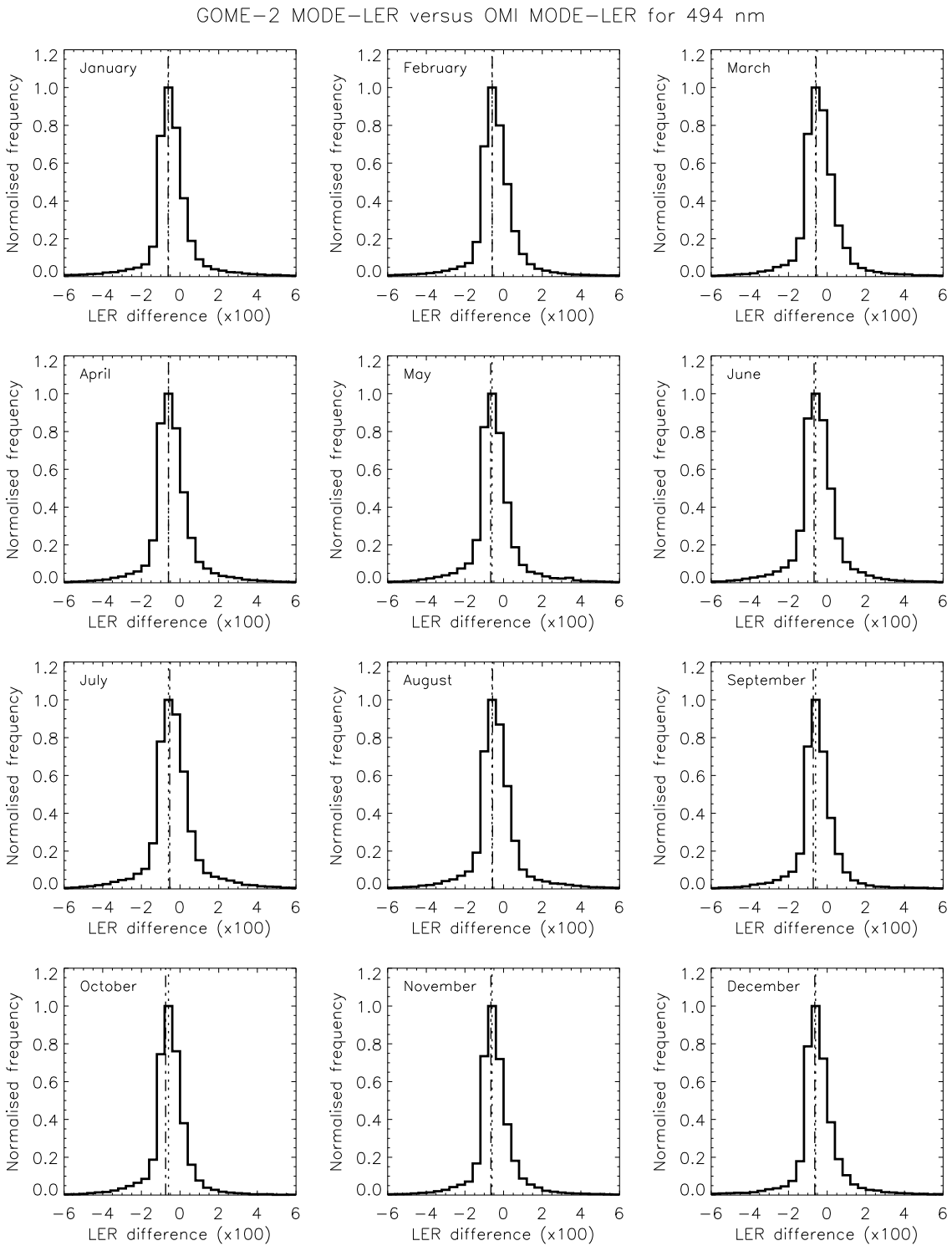

Figure 10: Histogram of the differences in the surface LER databases of GOME-2 and OMI at 494 nm. The MODE-LER products are compared. The agreement is very good. The vertical lines indicate the mean (dashed line) and the mode (dotted line) of the distribution.

GOME-2 versus OMI (MODE-LER)												
Mean surface LER difference ($\times$100)												
λ (nm)	JAN	FEB	MAR	APR	MAY	JUN	JUL	AUG	SEP	OCT	NOV	DEC
335	1.90	1.91	1.90	1.71	1.21	0.98	1.45	1.69	1.73	1.70	1.68	1.69
354	1.12	1.19	1.27	1.19	0.84	0.65	1.00	1.14	1.12	1.05	1.02	0.97
380	0.77	0.87	1.00	1.02	0.81	0.69	0.95	0.98	0.84	0.69	0.65	0.63
388	0.29	0.42	0.56	0.61	0.42	0.30	0.52	0.55	0.40	0.25	0.20	0.17
416	-0.23	-0.19	-0.16	-0.18	-0.39	-0.48	-0.26	-0.21	-0.28	-0.29	-0.25	-0.27
440	-0.55	-0.49	-0.48	-0.49	-0.65	-0.72	-0.49	-0.51	-0.61	-0.64	-0.60	-0.58
463	-0.62	-0.57	-0.55	-0.58	-0.69	-0.73	-0.54	-0.58	-0.69	-0.72	-0.66	-0.64
494	-0.62	-0.59	-0.57	-0.60	-0.67	-0.68	-0.54	-0.57	-0.72	-0.74	-0.65	-0.64
FWHM of distribution ($\times$100)												
λ (nm)	JAN	FEB	MAR	APR	MAY	JUN	JUL	AUG	SEP	OCT	NOV	DEC
335	2.31	2.13	2.17	2.15	2.13	2.20	2.29	2.30	2.21	2.28	2.32	2.35
354	2.15	2.03	2.06	1.99	1.96	2.07	2.19	2.13	2.12	2.19	2.21	2.19
380	2.07	2.02	2.23	2.24	2.01	2.14	2.30	2.21	2.22	2.27	2.21	2.17
388	1.98	1.94	2.14	2.17	1.93	2.05	2.22	2.12	2.13	2.18	2.13	2.09
416	1.69	1.75	1.88	1.80	1.69	1.70	1.79	1.76	1.67	1.73	1.77	1.79
440	1.58	1.67	1.79	1.75	1.61	1.72	1.82	1.75	1.61	1.62	1.64	1.66
463	1.42	1.50	1.60	1.60	1.52	1.60	1.72	1.58	1.46	1.47	1.47	1.48
494	1.28	1.38	1.46	1.42	1.35	1.47	1.55	1.42	1.28	1.26	1.25	1.28

Table 6: Mean difference in the surface LER of the GOME-2 and OMI surface LER databases. The FWHM of the distribution is also given. The numbers have been multiplied by 100.

the case for the width (FWHM) of the distributions, but also the mean and mode of the distributions are very comparable. This is a clear indication that the differences in the surface LER are mostly the result of differences in the two instruments, in the observation geometries, and in the time periods covered, but not so much in the retrieval approaches that are used. Note, however, that the differences that are found here are very small and that the conclusion to be drawn here is that the GOME-2 and OMI MODE-LER products are very much in agreement.

4.3 Conclusion of the comparison with OMI

The comparison with the OMI surface LER product as a reference indicates that the GOME-2 surface LER product is of good quality. Deviations are found, but these are small over the ocean and over most of the land. Near snow/ice borders we see differences, which may be explained by real differences in the actual snow/ice situation observed in the two observation periods (OMI: 2004–2007; GOME-2: 2007–2013). A bias in the surface LER difference is found over snow/ice surfaces. The bias is small and one cannot judge from the results whether the bias is caused by GOME-2, by OMI, or by the differences in overpass time and observation geometry. In summary, the GOME-2 MSC surface LER product has presented a high quality.

5 MSC-LER: Comparison with MERIS

In this section, we compare the GOME-2 surface LER product with the OMI black-sky albedo (BSA) product. Because a BSA is fundamentally different from a LER, differences are to be expected. Note that the MERIS BSA is only delivered for land surfaces. Over sea, the MERIS surface reflectivity that is present in the database is taken from the GOME-1 surface LER product. Nevertheless, the MERIS BSA may be useful as an independent reference.

We will compare the MERIS BSA with the GOME-2 MIN-LER and MODE-LER product, because it is not clear to us whether the MERIS surface reflectivity should be related to one or the other.

5.1 Global maps of the differences

In Figure 11 we plotted the difference between the GOME-2 MIN-LER and the MERIS BSA for the 772-nm wavelength band for the month March. In Figure 12 we do the same but here for GOME-2 the MODE-LER is used instead of the MIN-LER. For the sea surface, the conclusion is as expected: the differences are exactly the same as found in the comparison with GOME-1. For the land surfaces we see in the MIN-LER case that the difference is negative almost everywhere. For the MODE-LER case in Figure 12, there are also red areas (where the differences is positive).

In Figures 13 and 14 we repeat this but now for the 494-nm wavelength band. Here the differences are near-zero for large parts of the land surfaces. For the snow/ice covered land surfaces, however, the differences are negative. The MODE-LER comparison presented in Figure 14 reveals quite a few red areas, where the differences are positive. These areas have desert or snow/ice surfaces.

The conclusion is that we cannot draw much quantitative information from the comparison with the MERIS BSA. A statistical analysis will therefore not be presented. Note that a statistical analysis, when it would be performed, would be dominated by the sea surface.

5.2 Conclusion of the comparison with MERIS

The comparison with the MERIS BSA does not provide much additional information on the accuracy of the GOME-2 surface LER product. First of all, over sea the surface reflectivity values in the MERIS database are just those of the GOME-1 surface LER database. We compared the MERIS BSA with the GOME-2 MIN-LER and MODE-LER databases. The MERIS BSA over land appears to be systematically higher than the GOME-2 MIN-LER surface LER. On the other hand, for desert and snow/ice surfaces, the GOME-2 MODE-LER shows higher values than the MERIS database. A statistical analysis was not presented, because of the dominance of the sea surface.

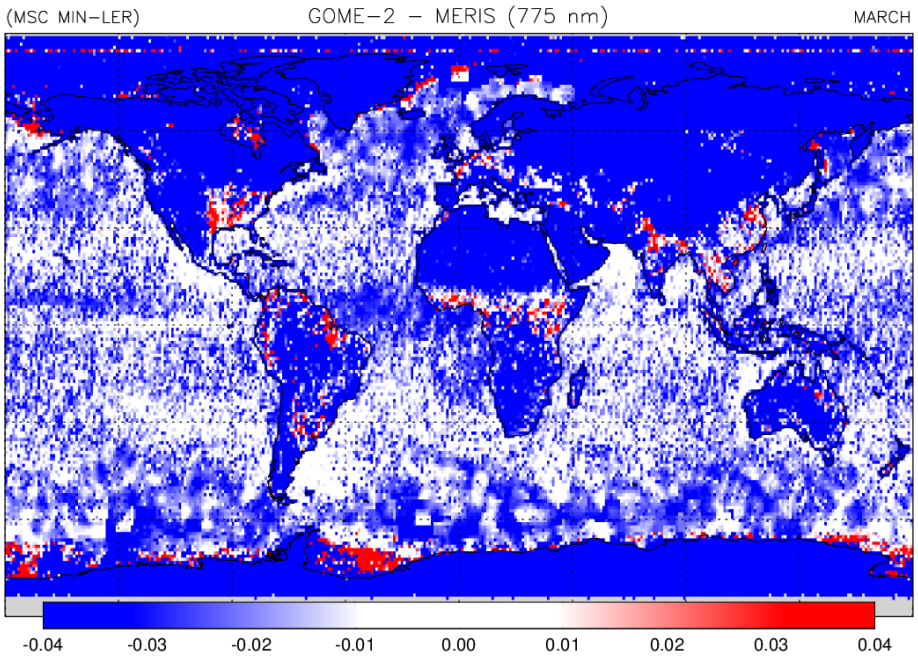

Figure 11: Map of the difference between the 772-nm surface LER from the GOME-2 and MERIS surface reflectivity databases for the month of March. The GOME-2 MIN-LER is plotted here. Please note that over the ocean, the MERIS database is filled with GOME-1 surface LER values.

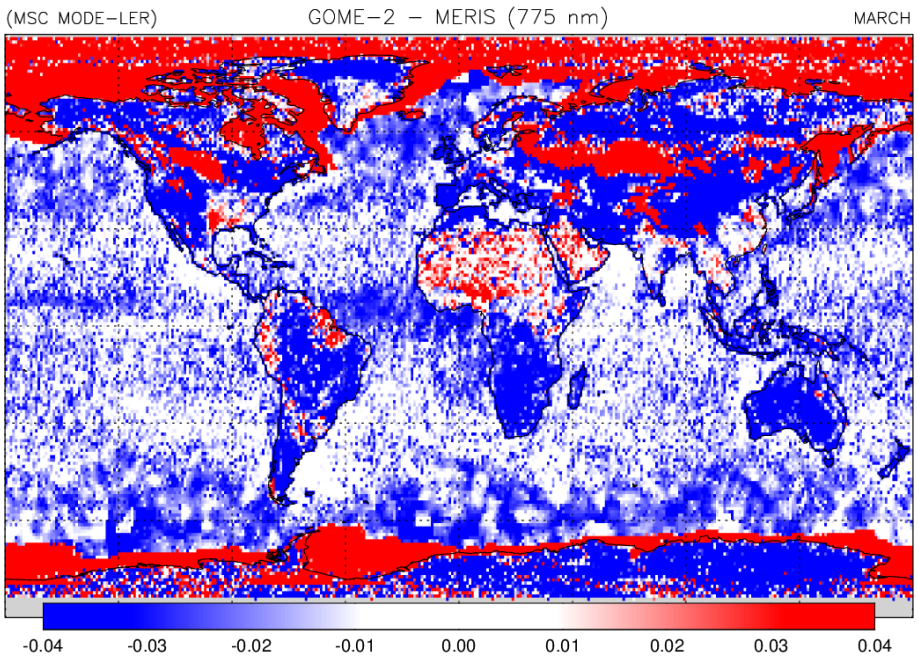

Figure 12: Map of the difference between the 772-nm surface LER from the GOME-2 and MERIS surface reflectivity databases for the month of March. The GOME-2 MODE-LER is plotted here. Please note that over the ocean, the MERIS database is filled with GOME-1 surface LER values.

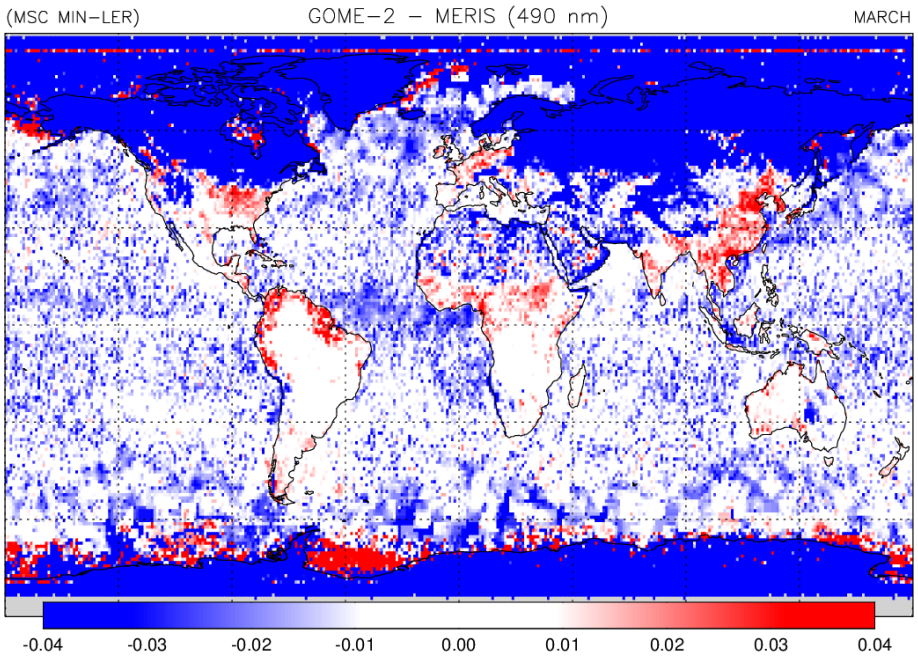

Figure 13: Map of the difference between the 494-nm surface LER from the GOME-2 and MERIS surface reflectivity databases for the month of March. The GOME-2 MIN-LER is plotted here. Please note that over the ocean, the MERIS database is filled with GOME-1 surface LER values.

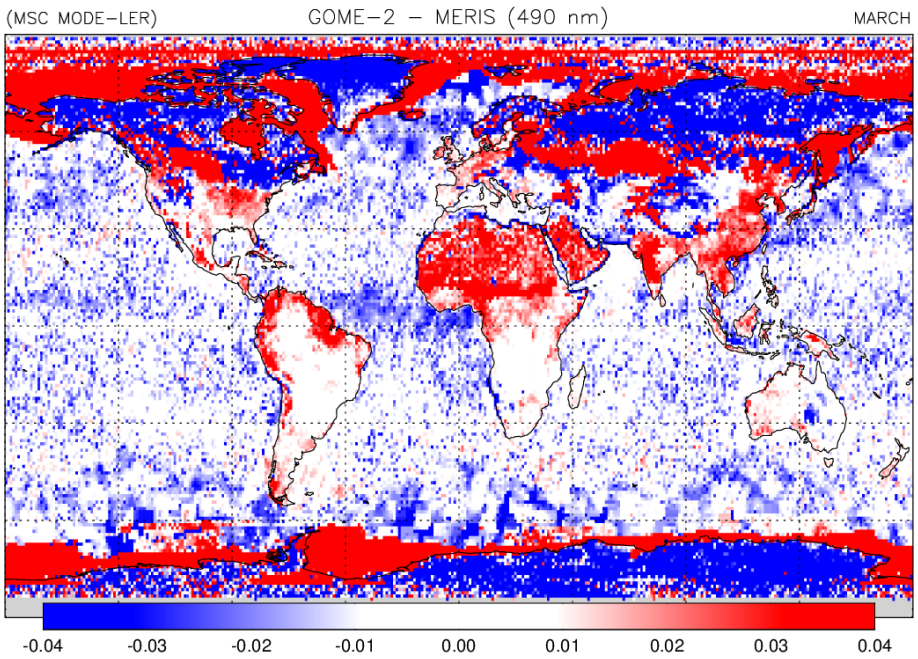

Figure 14: Map of the difference between the 494-nm surface LER from the GOME-2 and MERIS surface reflectivity databases for the month of March. The GOME-2 MODE-LER is plotted here. Please note that over the ocean, the MERIS database is filled with GOME-1 surface LER values.

6 PMD-LER: Comparison with OMI

For the GOME-2 PMD-LER product we do not perform a comparison with the GOME-1 surface LER product, for a number of reasons. First of all, the GOME-1 surface LER product is only available in the MIN-LER form. Secondly, the 335-nm and 380-nm GOME-1 surface LER wavelength bands are known to be affected by instrument degradation [*Koelemeijer et al.*, 2003]. Thirdly, the GOME-1 surface LER database has a lower spatial resolution (see Table 1). Fourthly, the GOME-1 surface LER wavelength bands are generally not close enough to the PMD wavelength bands. Using the OMI surface LER database makes more sense, as it has the same spatial resolution as the GOME-2 PMD surface LER product, is available in MIN-LER and MODE-LER versions, and has wavelength bands close enough to all PMD wavelength bands. The downside, unfortunately, is that the OMI wavelengths only go up to 499 nm. This means that we can only validate PMD bands 3–9.

6.1 Global maps of the differences

Global maps of the difference in surface LER are presented in Figures 15 and 16. Figure 15 presents the MIN-LER comparison for PMD 9; Figure 16 presents the MODE-LER comparison. The figures are very similar to the figures presented in section 4. There is, however, a bias of roughly 0.01 in the values over the ocean. This bias was not present for the MSC version. The most likely explanation is a difference in the radiometric calibration of the PMD band reflectance with respect to the MSC reflectance. Note that such differences have already been reported in the past [*Tilstra et al.*, 2011].

Over land the behaviour is not much different than over the ocean, except for the desert areas and the snow/ice areas. The behaviour over land is more or less in line with the behaviour over land that was seen for the MSC surface LER (see Figures 5 and 6). Note, however, that the closest wavelength band shown in these two figures was the 494 nm wavelength band whereas PMD 9 is centred around 461.3 nm and was compared with OMI wavelength band 463 nm. This difference of about 30 nm in wavelength may explain some of the differences between MSC-based LER and PMD-based LER.

6.2 Statistical analysis of the differences

In Figure 17 we present histograms of the difference between the GOME-2 MIN-LER product (for PMD 9) and the OMI MIN-LER (for the 463-nm wavelength band). In Figure 18 the same is presented, but then for the MODE-LER product. The mean and the width of the distributions for all PMD bands that could be validated (PMD 3–9) are summarised in Tables 7 and 8.

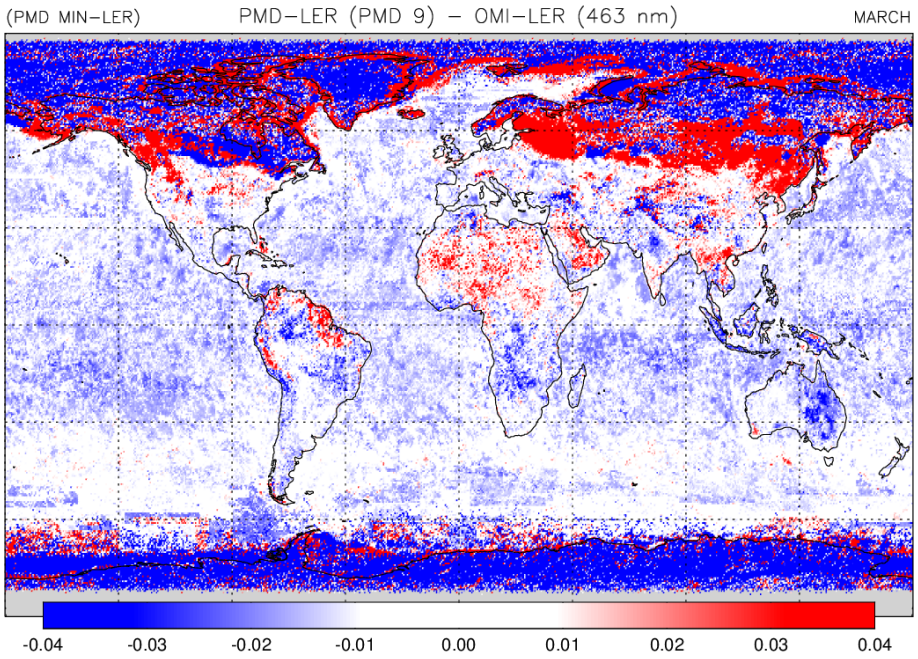

Figure 15: Map of the difference between the surface LER from GOME-2 (PMD 9) and OMI (463 nm). The MIN-LER is used here. Over the ocean, the agreement is good but with a negative bias of magnitude 0.01. Above snow/ice areas, the deviations are systematically larger.

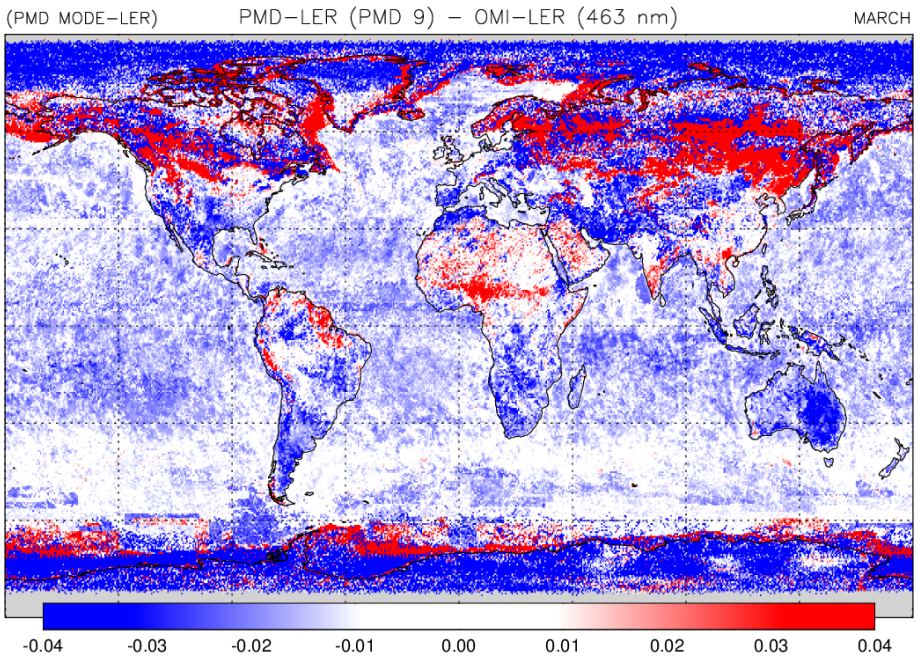

Figure 16: Map of the difference between the surface LER from GOME-2 (PMD 9) and OMI (463 nm). The MODE-LER is used here. Over the ocean, the agreement is good. Above land, the agreement is generally good, apart from differences related to snow/ice cover and extent.

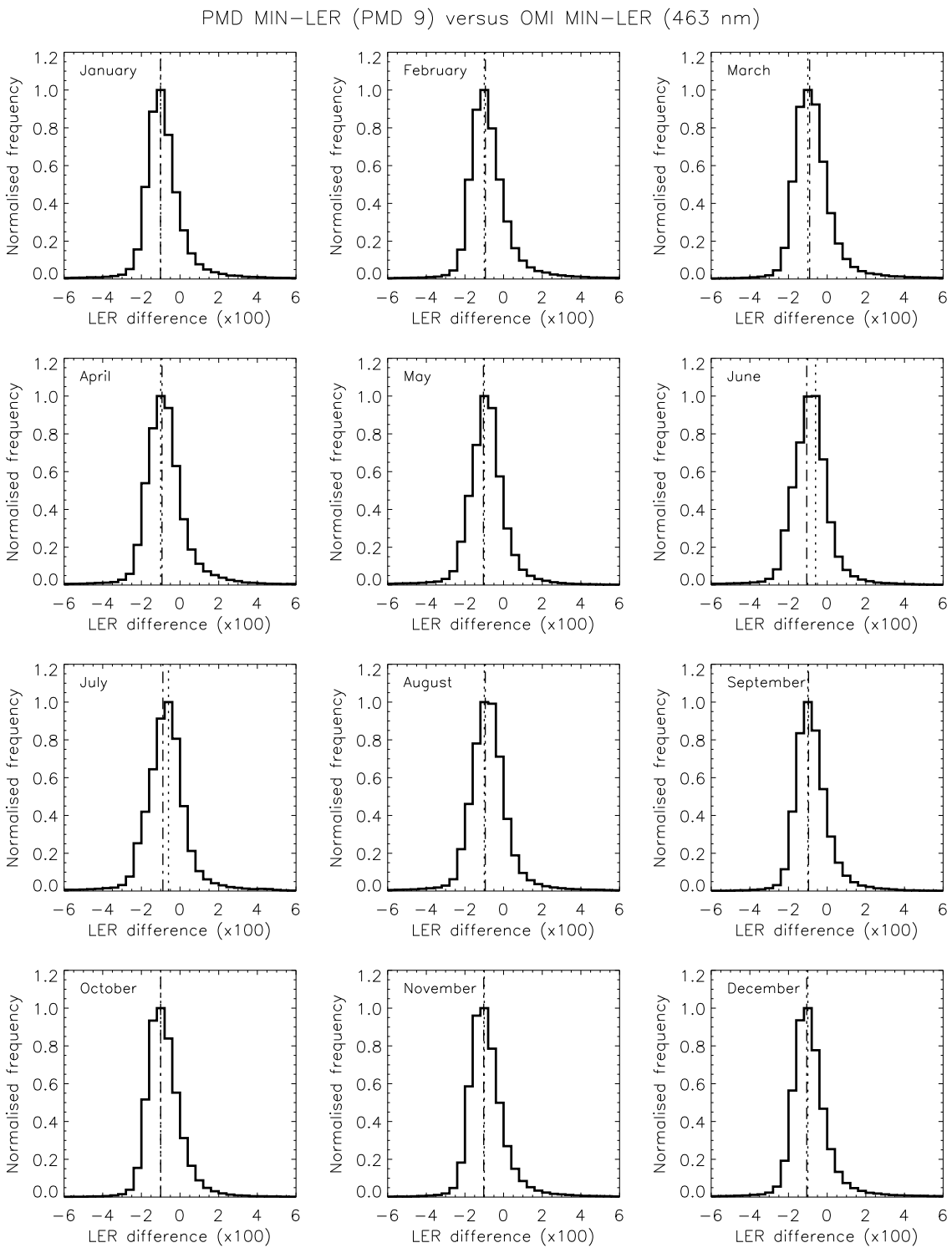

Figure 17: Histogram of the difference between the surface LER from GOME-2 (PMD 9) and OMI (463 nm). The MIN-LER products are compared. The agreement is good for all the months. The vertical lines indicate the mean (dashed line) and the mode (dotted line) of the distribution.

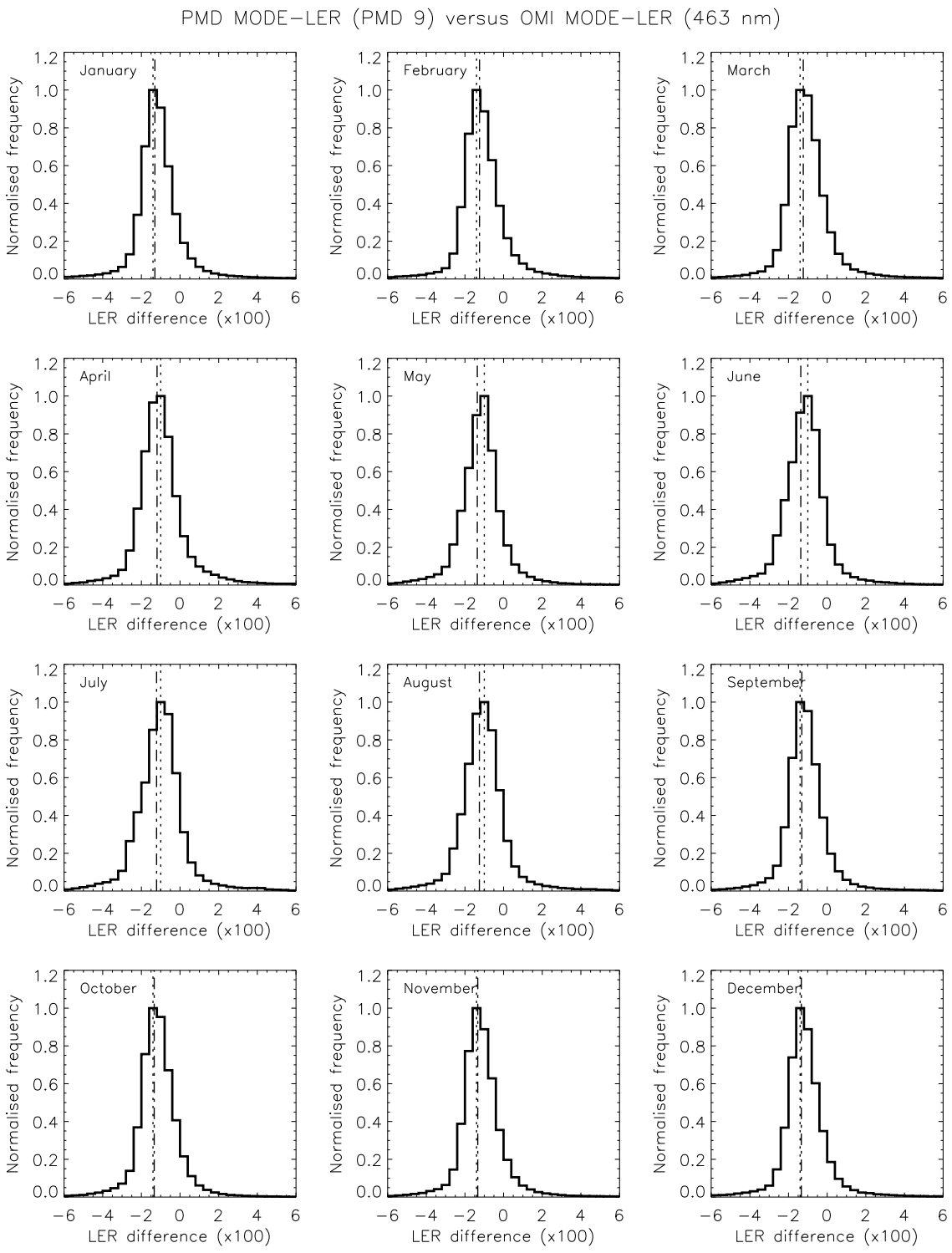

Figure 18: Histogram of the difference between the surface LER from GOME-2 (PMD 9) and OMI (463 nm). The MODE-LER products are compared. The agreement is very good. The vertical lines indicate the mean (dashed line) and the mode (dotted line) of the distribution.

GOME-2 versus OMI (MIN-LER)												
Difference in surface LER ($\times$100)												
PMD	JAN	FEB	MAR	APR	MAY	JUN	JUL	AUG	SEP	OCT	NOV	DEC
3	3.09	3.08	3.13	3.11	3.09	3.07	3.06	2.97	3.06	3.13	3.07	3.03
4	-2.21	-2.35	-2.38	-2.46	-2.51	-2.55	-2.23	-2.37	-2.44	-2.36	-2.35	-2.29
5	-2.36	-2.42	-2.45	-2.47	-2.52	-2.58	-2.45	-2.56	-2.58	-2.50	-2.46	-2.46
6	-0.42	-0.42	-0.41	-0.44	-0.48	-0.51	-0.42	-0.50	-0.45	-0.41	-0.44	-0.47
7	-1.53	-1.54	-1.51	-1.52	-1.58	-1.58	-1.40	-1.52	-1.53	-1.54	-1.60	-1.62
8	-0.92	-0.87	-0.83	-0.86	-0.96	-0.97	-0.85	-0.91	-0.90	-0.93	-0.97	-1.00
9	-1.01	-0.94	-0.91	-0.93	-1.04	-1.06	-0.89	-0.95	-0.96	-1.00	-1.03	-1.06
FWHM of distribution ($\times$100)												
PMD	JAN	FEB	MAR	APR	MAY	JUN	JUL	AUG	SEP	OCT	NOV	DEC
3	3.28	3.55	3.89	4.23	4.01	4.17	4.19	3.80	4.08	4.24	3.78	3.55
4	2.44	2.63	2.60	2.62	2.76	2.85	2.73	2.52	2.58	2.55	2.50	2.43
5	2.35	2.49	2.51	2.61	2.77	2.79	2.83	2.54	2.48	2.40	2.38	2.32
6	2.19	2.20	2.26	2.40	2.46	2.45	2.50	2.34	2.19	2.24	2.31	2.28
7	1.99	2.02	2.06	2.16	2.22	2.25	2.24	2.11	1.98	2.05	2.10	2.04
8	2.00	2.07	2.12	2.17	2.12	2.11	2.18	2.09	1.92	2.05	2.08	2.05
9	1.60	1.70	1.77	1.82	1.74	1.82	1.90	1.81	1.61	1.70	1.67	1.64

Table 7: Mean difference in the surface LER of the GOME-2 PMD-LER and OMI surface LER databases. The FWHM of the distribution is also given. The numbers have been multiplied by 100.

GOME-2 versus OMI (MODE-LER)												
Difference in surface LER ($\times$100)												
PMD	JAN	FEB	MAR	APR	MAY	JUN	JUL	AUG	SEP	OCT	NOV	DEC
3	3.08	2.99	3.06	3.09	3.10	3.12	3.05	2.93	2.97	3.10	3.05	3.04
4	-2.46	-2.67	-2.72	-2.78	-2.82	-2.83	-2.52	-2.67	-2.76	-2.72	-2.66	-2.58
5	-2.61	-2.73	-2.78	-2.78	-2.81	-2.84	-2.72	-2.85	-2.88	-2.83	-2.76	-2.74
6	-0.66	-0.70	-0.69	-0.65	-0.72	-0.74	-0.67	-0.74	-0.73	-0.70	-0.72	-0.74
7	-1.83	-1.85	-1.83	-1.81	-1.90	-1.87	-1.71	-1.83	-1.85	-1.86	-1.90	-1.90
8	-1.22	-1.18	-1.16	-1.12	-1.28	-1.28	-1.17	-1.21	-1.24	-1.26	-1.28	-1.29
9	-1.30	-1.25	-1.24	-1.19	-1.36	-1.36	-1.21	-1.25	-1.31	-1.34	-1.34	-1.34
FWHM of distribution ($\times$100)												
PMD	JAN	FEB	MAR	APR	MAY	JUN	JUL	AUG	SEP	OCT	NOV	DEC
3	3.24	3.54	3.76	3.89	3.77	3.88	3.99	3.79	4.08	4.25	3.80	3.53
4	2.17	2.41	2.43	2.45	2.62	2.67	2.64	2.40	2.44	2.36	2.29	2.17
5	2.15	2.31	2.37	2.47	2.69	2.70	2.73	2.43	2.34	2.25	2.22	2.12
6	2.21	2.19	2.21	2.32	2.39	2.39	2.46	2.31	2.16	2.19	2.29	2.25
7	1.98	1.96	1.96	2.03	2.12	2.15	2.20	2.06	1.90	1.94	2.02	1.97
8	2.04	2.12	2.16	2.23	2.19	2.19	2.29	2.21	1.99	2.07	2.11	2.07
9	1.67	1.78	1.84	1.91	1.84	1.96	2.07	1.96	1.71	1.76	1.74	1.70

Table 8: Mean difference in the surface LER of the GOME-2 PMD-LER and OMI surface LER databases. The FWHM of the distribution is also given. The numbers have been multiplied by 100.

6.3 Conclusion of the comparison with OMI

The PMD-based version of the GOME-2 surface LER compares well to the OMI surface LER. This holds for both the MIN-LER and MODE-LER versions. In the comparison a small mismatch between the wavelengths of the PMD bands and the OMI wavelength bands had to be accepted. This, and the different wavelength width of the PMD bands, will have had an impact on the outcome of the comparison. Nevertheless, the results indicate that the PMD-LER is in general of good quality. Over sea a small difference of -0.01 is found in comparison to OMI. Over snow/ice surfaces there are larger differences, which are still acceptable, and may be explained by differences in radiometric calibration of the PMDs. The existence of such differences is not speculative as these have already been reported in the past [*Tilstra et al.*, 2011]. All in all, the PMD-LER is found to be of good quality.

7 PMD-LER versus MSC-LER

In this section we compare the GOME-2 PMD-LER database to the GOME-2 MSC-LER database. As both algorithms are to a high degree equal, differences found must be attributed to differences related to performance (footprint size, number of observations per month), differences related to the time periods covered, differences related to the wavelength mismatch between PMD band and MSC wavelength band, or to differences related to the radiometric calibration of PMDs and MSCs.

As a result of too large wavelength mismatches between some of the PMD bands and their MSC counterparts, we can only validate PMD bands 3–9, 11–12, and 14.

7.1 Global maps of the differences

In Figure 19 we present a global map of the difference between the MIN-LER of the PMD-LER and the MIN-LER of the MSC-LER, for the month March. Here we compare the PMD-LER from PMD 11 (centred around 555 nm) with the MSC-LER wavelength band located at 555 nm. Note that PMD 11 is a relatively thin PMD band [*EUMETSAT*, 2014], which makes the comparison more accurate. From Figure 19 we conclude that there is a high agreement between the PMD-LER and the MSC-LER. Only for areas that may be linked to high values of the surface albedo (snow/ice areas) there is a clear negative difference. The difference goes up to 0.04 in magnitude. The most likely explanation is difference in the calibration of PMD bands and the main science channels.

Other differences that are worth noting are the appearance of features related to residual cloud contamination (over the seas surrounding Antarctica) and features related to snow/ice presence and extent. The residual cloud features are modest, with differences up to up to 0.02 in magnitude. Nevertheless, the appearance of these features illustrates the better handling of these situations by the PMD-based surface LER, as expected. The “red” areas in Eurasia shown in Figure 19 are related to snow/ice presence. This difference is caused by the different time periods used for the PMD-LER and the MSC-LER. To explain, the MSC-LER for the month March is based on data from the years 2007–2013. The PMD-LER is based on data from the years 2009–2013. The red areas indicate that for the month March in the years 2007–2008 there was a period when there was no snow/ice presence in these areas. This results in no snow in the MSC MIN-LER, but snow in the PMD MIN-LER.

If this explanation (which was checked by looking at the MSC MIN-LER based on the individual years) is correct, then the snow/ice feature should not be present in the MODE-LER difference plot. Indeed, in Figure 20, which presents the surface LER difference based using the MODE-LER approach, the “red” features are absent. These observations support the claim by *Kleipool et al.* [2008] that the MODE-LER is the more representative surface LER database for snow/ice areas.

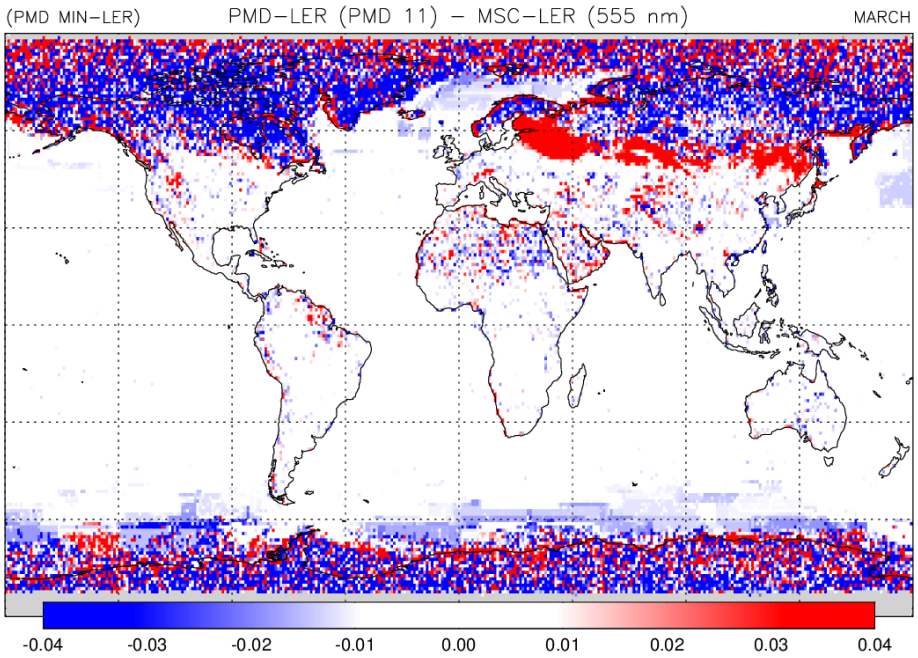

Figure 19: Map of the difference between the surface LER from the GOME-2 PMD-LER (PMD 11) and the GOME-2 MSC-LER (555 nm). The MIN-LER is plotted here, for the month of March.

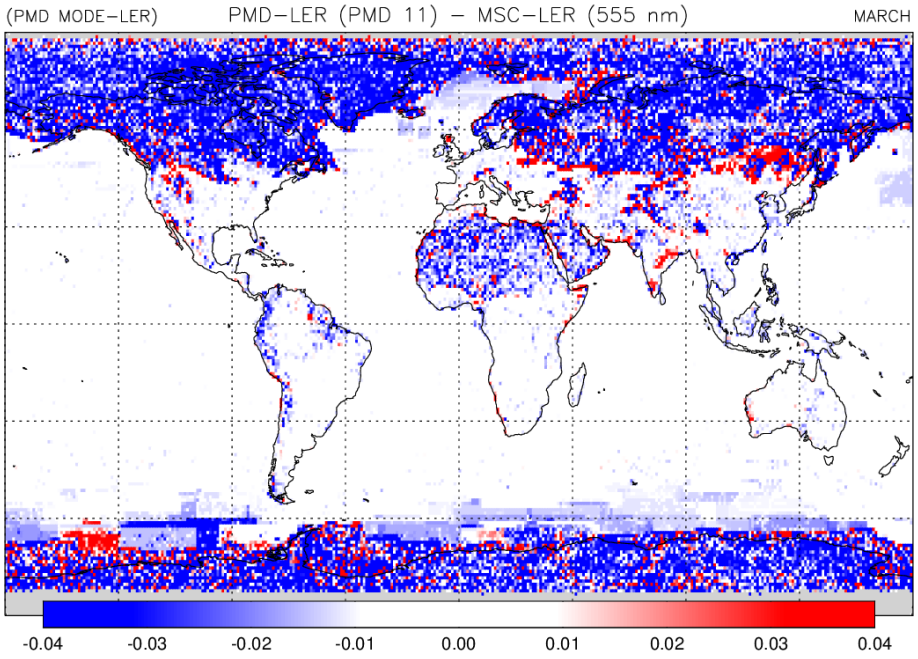

Figure 20: Map of the difference between the surface LER from the GOME-2 PMD-LER (PMD 11) and the GOME-2 MSC-LER (555 nm). The MODE-LER is plotted here, for the month of March.

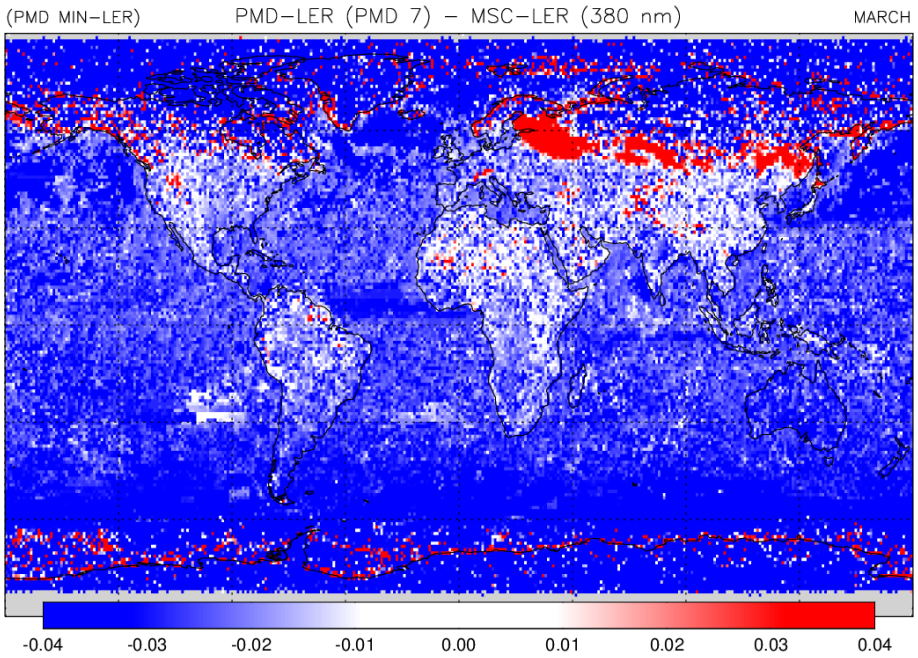

Figure 21: Map of the difference between the surface LER from the GOME-2 PMD-LER (PMD 7) and the GOME-2 MSC-LER (380 nm). The MIN-LER is plotted here, for the month of March.

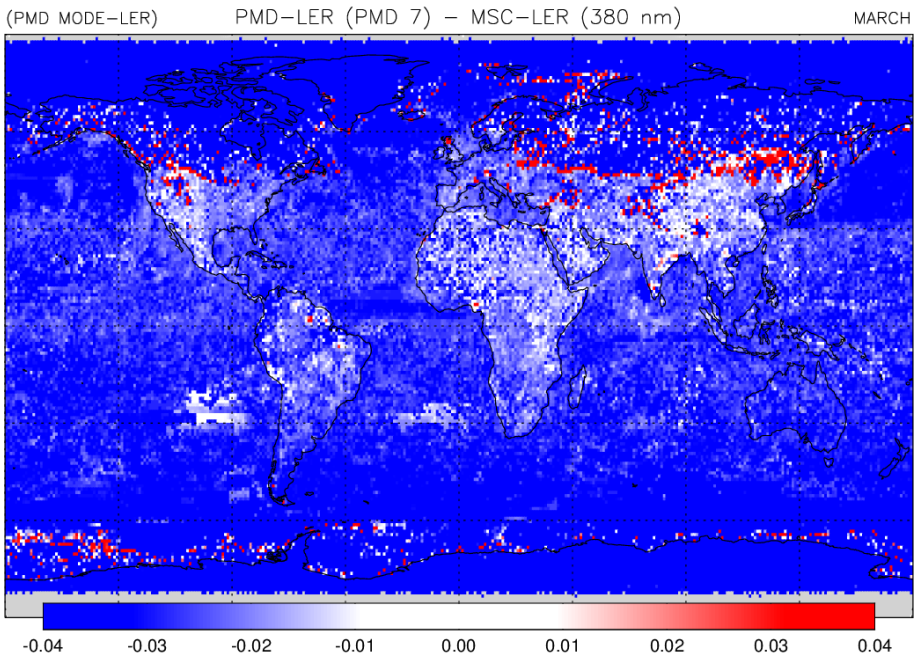

Figure 22: Map of the difference between the surface LER from the GOME-2 PMD-LER (PMD 7) and the GOME-2 MSC-LER (380 nm). The MODE-LER is plotted here, for the month of March.

In Figures 21 and 20 we present similar plots but now based on the comparison between PMD 7 (centred around 383 nm) and the MSC wavelength band located at 380 nm. This time the differences are larger over both sea and land. Note that PMD 7 was selected here mainly because of its thin bandwidth [*EUMETSAT*, 2014]. The difference (going up to 0.04 in magnitude) must be caused by differences in radiometric calibration. Note that relative errors of up to 4% were reported in the past for the PMD bands [*Tilstra et al.*, 2011]. To be more precise, for PMD 7 the "transformation" from MSC to PMD that was found was $R_{\mathrm{PMD7}} \approx 0.98 \cdot R_{\mathrm{MSC}} - 0.01$. Such a relationship between MSC reflectance and measured PMD reflectance would explain a surface LER difference of -0.03 for snow surfaces (assuming an albedo of 0.8). For the desert areas (albedo around 0.2), the error explained would be around -0.014. For the ocean (albedo around 0.03), the error explained would be around -0.01. These numbers are in the range of what we see in Figures 21 and 20. Note that the PMD-LER may also be partly lower than the MSC-LER because of the better statistics involved, i.e., the higher chances of finding cloud-free scenes may lead to somewhat lower values for the PMD-LER.

7.2 Statistical analysis of the differences

In Figures 23 and 24 we present histograms of the surface LER differences for PMD 11 for all twelve months of the year. The MIN-LER differences are presented in Figure 23 and the MODE-LER differences are presented in Figure 24. The agreement is high. No seasonal dependence is observed. In Figures 25 and 26 we present the results for PMD 7. Here we find, as expected and as discussed earlier, larger differences. A large seasonal variation is again not present.

In Tables 9 and 10 we present the difference between PMD-LER and MSC-LER for all PMD bands that could be compared and for all months. The results for the MIN-LER comparison are presented in Table 9 and the ones for the MODE-LER comparison are presented in Table 10.

7.3 Conclusion of the PMD-LER versus MSC-LER comparison

In general, the agreement between PMD-LER and MSC-LER is high. For the shorter wavelengths the difference is, however, larger and increasing with decreasing wavelength. We attribute these differences mainly to imperfections in the radiometric calibration of the PMD bands. From earlier studies [*Tilstra et al.*, 2011] we know of the existence of such calibration issues for the PMD band reflectances. When we take the reported calibration errors of the PMD bands into account and calculate the impact for the different surface types we can reproduce the differences that were found between PMD-LER and MSC-LER. Therefore, the radiometric calibration explains most of the differences found. Note that the PMD-LER and MSC-LER retrieval codes are for a large part identical.

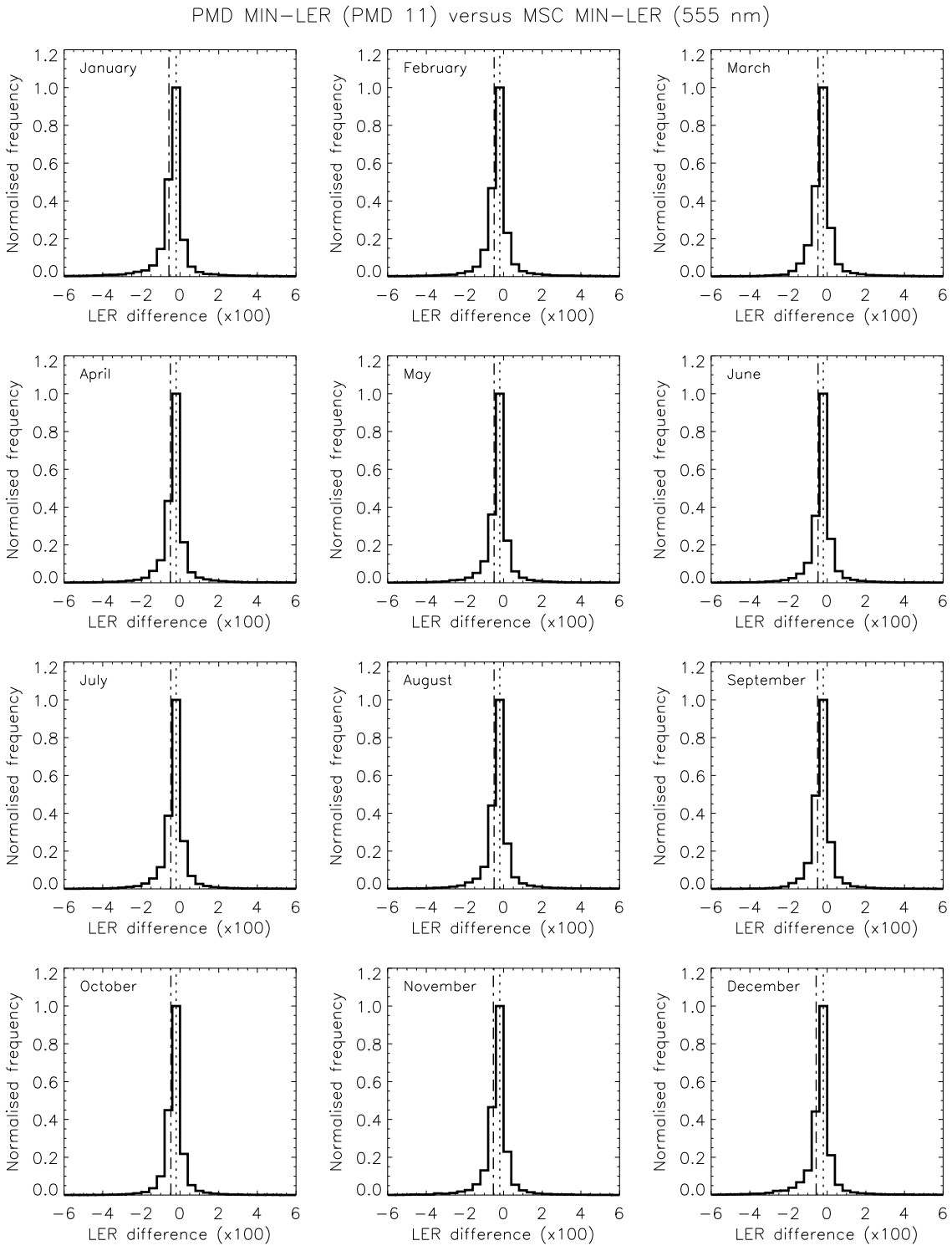

Figure 23: Histogram of the difference between the surface LER from the GOME-2 PMD-LER (PMD 11) and the GOME-2 MSC-LER (555 nm). The MIN-LER products for March are compared. The vertical lines indicate the mean (dashed line) and the mode (dotted line) of the distribution.

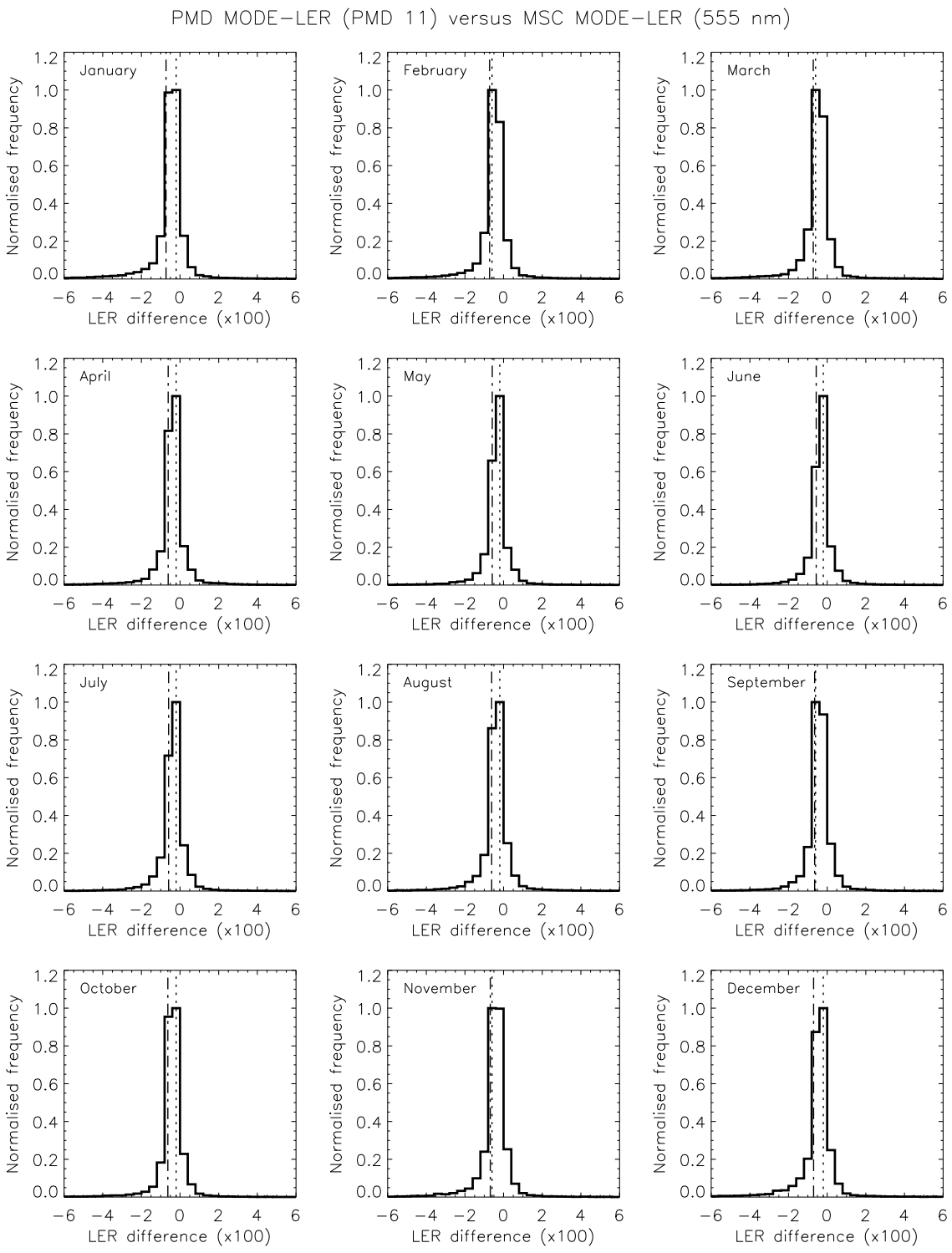

Figure 24: Histogram of the difference between the surface LER from the GOME-2 PMD-LER (PMD 11) and the GOME-2 MSC-LER (555 nm). The MODE-LER products for March are compared. The vertical lines indicate the mean (dashed line) and the mode (dotted line) of the distribution.

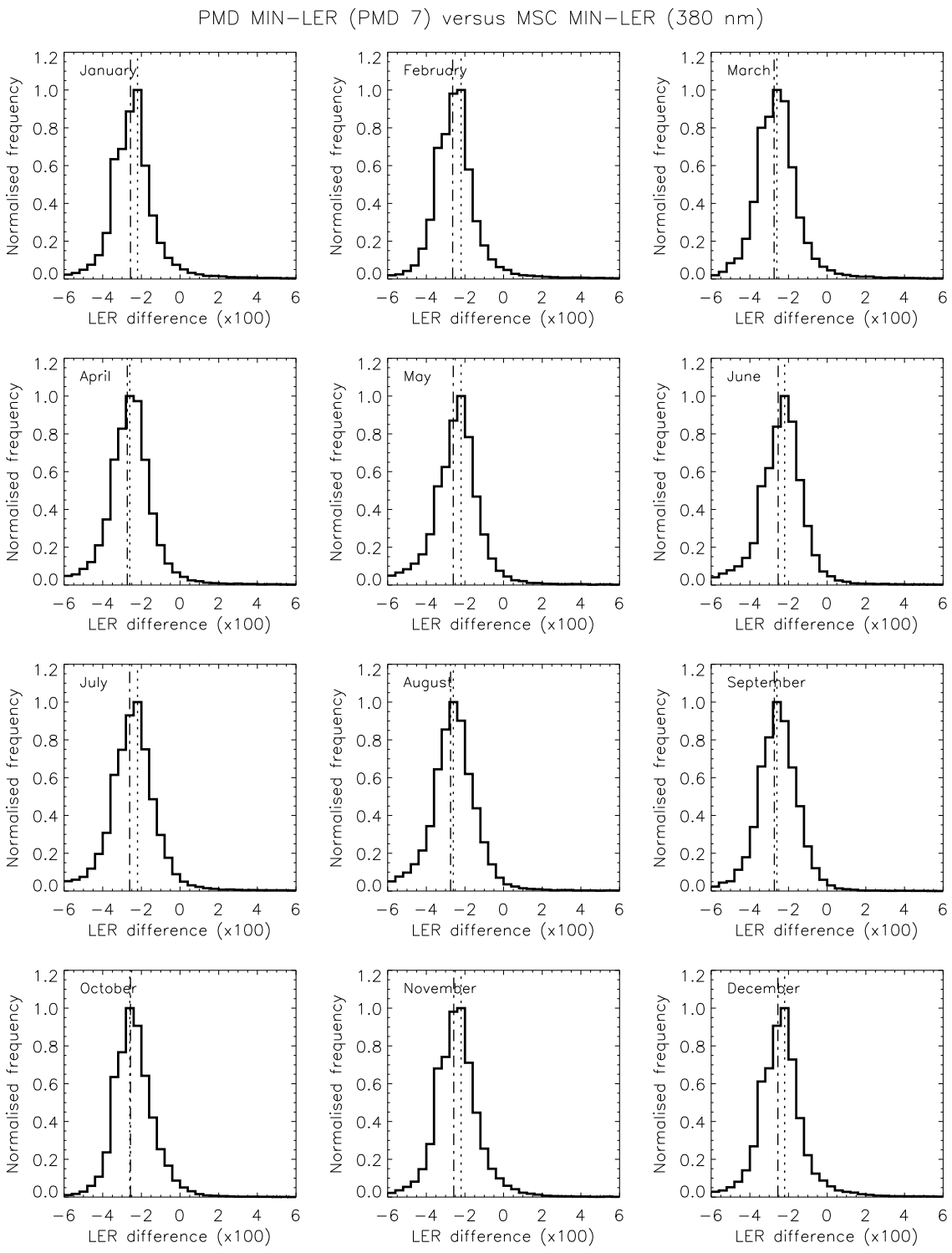

Figure 25: Histogram of the difference between the surface LER from the GOME-2 PMD-LER (PMD 7) and the GOME-2 MSC-LER (380 nm). The MIN-LER products for March are compared. The vertical lines indicate the mean (dashed line) and the mode (dotted line) of the distribution.

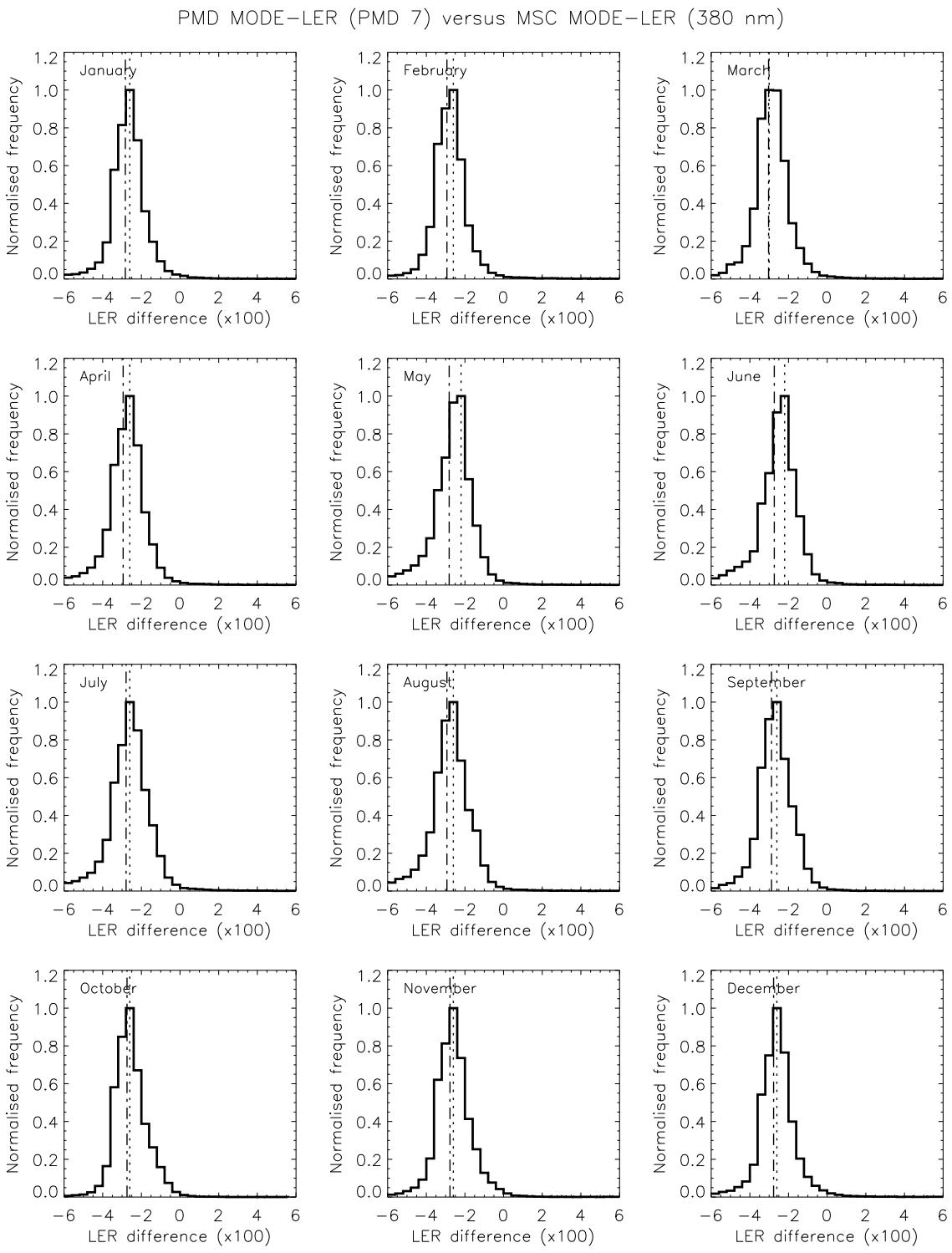

Figure 26: Histogram of the difference between the surface LER from the GOME-2 PMD-LER (PMD 7) and the GOME-2 MSC-LER (380 nm). The MODE-LER products for March are compared. The vertical lines indicate the mean (dashed line) and the mode (dotted line) of the distribution.

GOME-2 PMD-LER versus MSC-LER (MIN-LER)												
Difference in surface LER ($\times$100)												
PMD	JAN	FEB	MAR	APR	MAY	JUN	JUL	AUG	SEP	OCT	NOV	DEC
3	-3.74	-3.77	-3.86	-3.69	-3.28	-3.13	-3.49	-3.80	-4.00	-3.89	-3.73	-3.68
4	-4.12	-4.23	-4.27	-4.17	-3.88	-3.77	-3.83	-4.14	-4.29	-4.20	-4.12	-4.08
5	-3.81	-3.93	-4.00	-3.87	-3.54	-3.45	-3.66	-3.95	-4.09	-3.97	-3.89	-3.82
7	-2.57	-2.64	-2.75	-2.73	-2.60	-2.54	-2.61	-2.74	-2.73	-2.57	-2.58	-2.55
8	-1.08	-1.01	-1.02	-1.01	-0.93	-0.85	-0.96	-1.04	-1.07	-1.06	-1.14	-1.12
9	-0.78	-0.71	-0.71	-0.72	-0.71	-0.69	-0.68	-0.71	-0.72	-0.70	-0.78	-0.80
11	-0.57	-0.49	-0.48	-0.50	-0.49	-0.47	-0.48	-0.49	-0.49	-0.47	-0.53	-0.57
12	-0.39	-0.30	-0.31	-0.36	-0.35	-0.34	-0.34	-0.35	-0.33	-0.32	-0.35	-0.40
14	-0.87	-0.78	-0.80	-0.88	-0.94	-0.97	-0.95	-0.94	-0.92	-0.87	-0.88	-0.89
FWHM of distribution ($\times$100)												
PMD	JAN	FEB	MAR	APR	MAY	JUN	JUL	AUG	SEP	OCT	NOV	DEC
3	3.79	3.88	3.71	3.48	3.46	3.64	3.70	3.66	3.68	3.84	3.93	3.83
4	2.38	2.63	2.50	2.37	2.46	2.44	2.52	2.65	2.63	2.57	2.80	2.55
5	2.29	2.38	2.35	2.29	2.46	2.42	2.54	2.52	2.48	2.42	2.66	2.60
7	1.99	1.97	2.11	2.12	2.15	2.16	2.28	2.23	2.17	2.06	2.14	2.09
8	1.26	1.36	1.43	1.26	1.25	1.30	1.30	1.26	1.22	1.24	1.41	1.36
9	0.91	0.97	0.97	0.89	0.98	0.99	1.02	0.99	0.90	0.87	0.94	0.98
11	0.65	0.65	0.68	0.62	0.60	0.60	0.63	0.64	0.67	0.63	0.65	0.63
12	0.72	0.74	0.77	0.68	0.71	0.71	0.71	0.73	0.75	0.72	0.73	0.71
14	0.52	0.53	0.55	0.48	0.49	0.48	0.50	0.51	0.53	0.51	0.52	0.51

Table 9: Mean difference in the surface LER of the GOME-2 PMD and MSC surface LER databases. The FWHM of the distribution is also given. The numbers have been multiplied by 100.

GOME-2 PMD-LER versus MSC-LER (MODE-LER)												
Difference in surface LER ($\times$100)												
PMD	JAN	FEB	MAR	APR	MAY	JUN	JUL	AUG	SEP	OCT	NOV	DEC
3	-4.07	-4.20	-4.30	-4.06	-3.61	-3.43	-3.81	-4.07	-4.35	-4.34	-4.19	-4.08
4	-4.54	-4.65	-4.65	-4.49	-4.18	-4.04	-4.07	-4.40	-4.53	-4.50	-4.44	-4.46
5	-4.20	-4.33	-4.36	-4.16	-3.81	-3.69	-3.90	-4.21	-4.31	-4.24	-4.18	-4.17
7	-2.83	-2.93	-3.03	-2.94	-2.81	-2.74	-2.79	-2.93	-2.88	-2.74	-2.77	-2.77
8	-1.21	-1.22	-1.22	-1.13	-1.06	-0.98	-1.07	-1.17	-1.18	-1.18	-1.26	-1.24
9	-0.88	-0.89	-0.89	-0.82	-0.79	-0.78	-0.77	-0.82	-0.82	-0.82	-0.89	-0.90
11	-0.72	-0.72	-0.72	-0.61	-0.59	-0.57	-0.59	-0.62	-0.65	-0.63	-0.69	-0.70
12	-0.54	-0.52	-0.53	-0.47	-0.46	-0.44	-0.46	-0.46	-0.47	-0.46	-0.51	-0.53
14	-0.96	-0.94	-0.97	-0.99	-1.05	-1.13	-1.11	-1.09	-1.08	-1.01	-1.01	-0.99
FWHM of distribution ($\times$100)												
PMD	JAN	FEB	MAR	APR	MAY	JUN	JUL	AUG	SEP	OCT	NOV	DEC
3	3.21	3.29	3.09	2.77	2.67	2.78	2.91	3.02	3.04	3.16	3.30	3.17
4	2.07	2.27	2.24	2.04	1.96	1.92	2.10	2.30	2.30	2.23	2.33	2.12
5	1.98	2.07	2.05	1.94	1.96	1.91	2.12	2.21	11.14	2.10	2.21	2.07
7	1.58	1.58	1.65	1.74	1.81	1.76	1.94	1.89	1.80	1.69	1.71	1.60
8	1.01	1.11	1.14	0.98	0.89	0.93	1.01	1.02	0.98	0.96	1.10	1.06
9	0.84	0.95	0.88	0.75	0.77	0.79	0.88	0.84	0.79	0.77	0.87	0.89
11	0.79	0.80	0.81	0.75	0.71	0.69	0.77	0.80	0.81	0.76	0.81	0.80
12	0.64	0.63	0.63	0.57	0.57	0.60	0.60	0.62	0.65	0.65	0.66	0.65
14	0.57	0.60	0.60	0.54	0.54	0.55	0.57	0.58	0.62	0.58	0.60	0.58

Table 10: Mean difference in the surface LER of the GOME-2 PMD and MSC surface LER databases. The FWHM of the distribution is also given. The numbers have been multiplied by 100.

For the MIN-LER database, we found a difference between PMD-LER and MSC-LER that was caused by a difference in snow/ice presence due to the different time periods that were observed. This difference was not present in the MODE-LER database. This confirms that the MODE-LER approach is better suited to handle snow/ice surfaces.

8 Summary

By direct comparison with the GOME-1 and OMI surface LER databases we conclude that the GOME-2 MSC MIN-LER and the GOME-2 MSC MODE-LER surface LER products are accurate within 0.01 over the ocean and accurate within 0.04 over snow/ice surfaces. These numbers are valid under the assumption that the most important reference used here (the OMI surface LER product) is perfect. Differences in overpass time and observation geometry have a clear impact on the retrieved surface LER. From this point of view, the small difference found from the comparisons must be regarded as a clear indication that the GOME-2 surface LER products have a high quality.

As for the GOME-2 PMD-based surface LER, we were only able to validate the surface LER from the PMD bands up to PMD 9. The results indicate that the PMD-LER is reliable. Over the ocean there appears to be a bias of 0.01, depending on PMD/wavelength. Over land the differences are again higher, as was the case for the MSC-based LER. The differences are most likely caused by differences in radiometric calibration of the PMDs. The existence of such radiometric calibration differences is not speculative as these have already been reported in the past [*Tilstra et al.*, 2011].

A comparison between PMD-LER and MSC-LER shows that there is a good agreement for the higher PMD bands, but a less good agreement for the lower PMD bands. We attribute the differences that are found mainly to calibration issues. All in all, the PMD-LER is found to be of good quality.

A Examples of the monthly GOME-2 surface LER product

The following figures present global maps of the GOME-2 surface LER (MODE-LER approach) retrieved at 772 nm for the months January to December. (Continued on next page.)

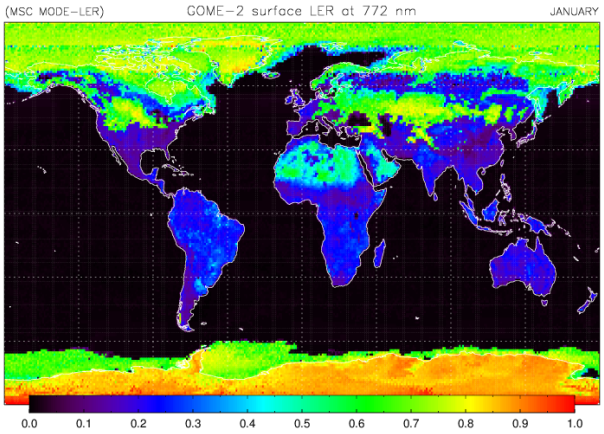

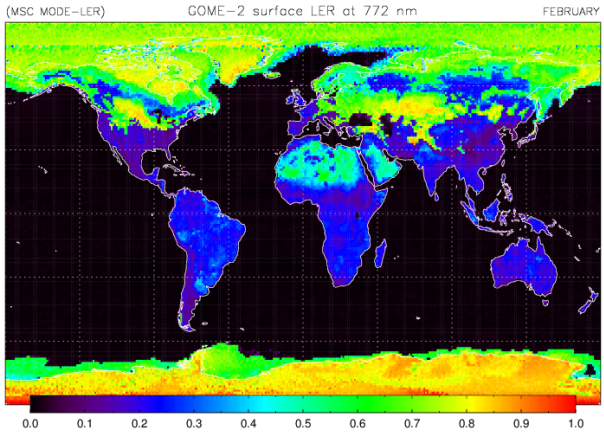

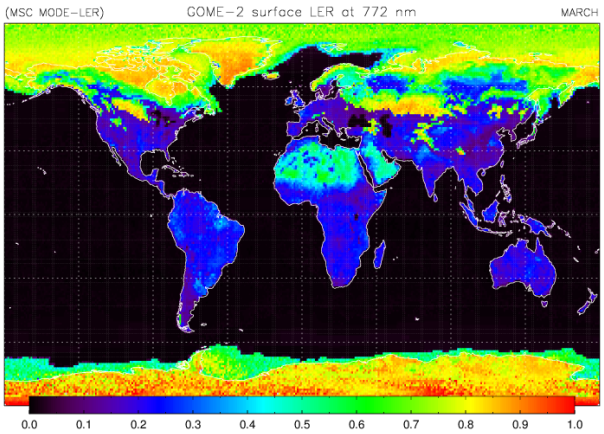

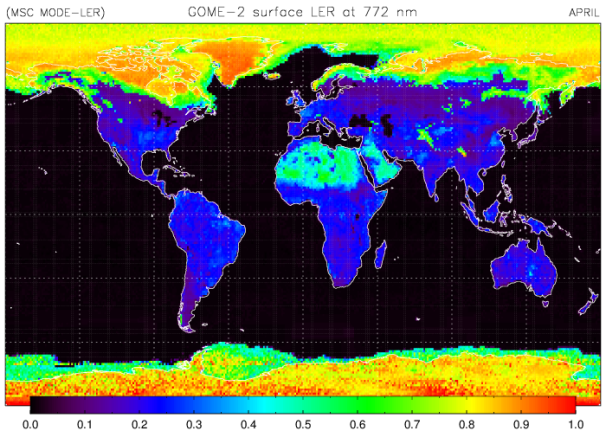

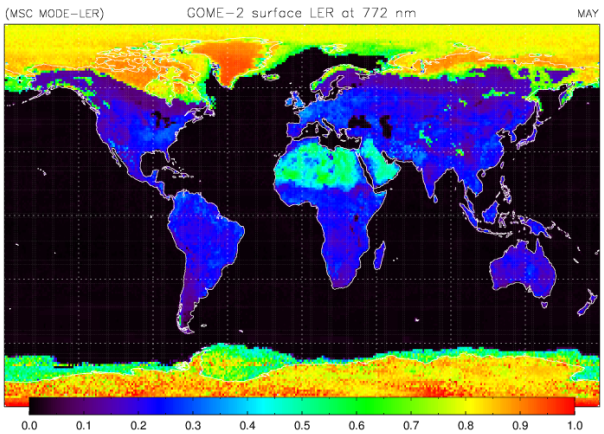

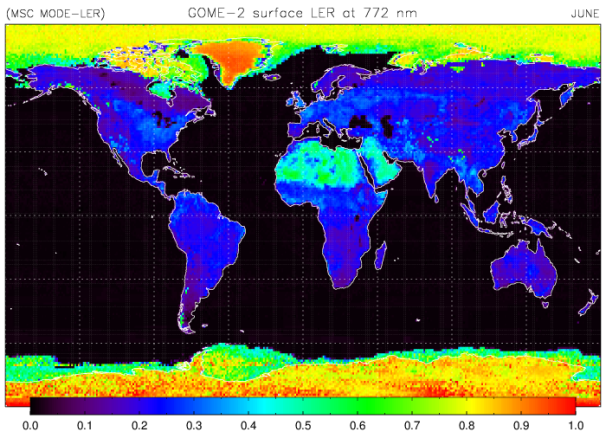

(Continued from previous page.)

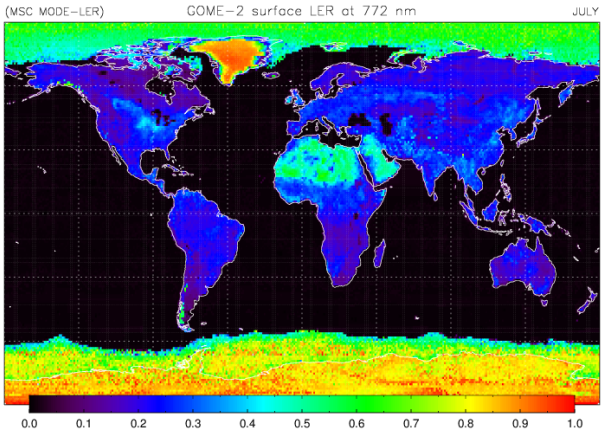

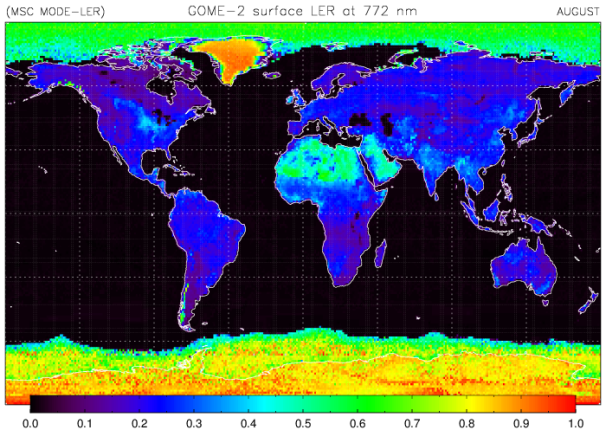

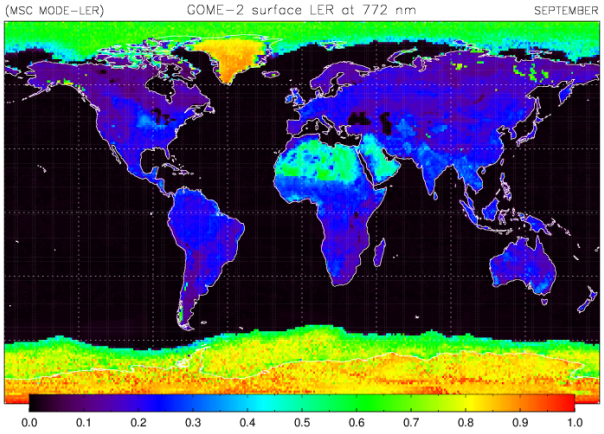

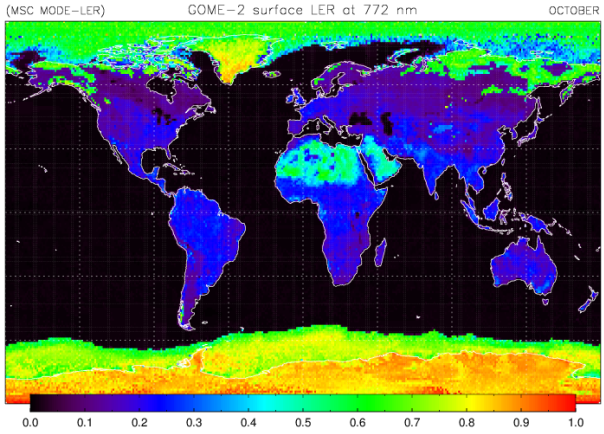

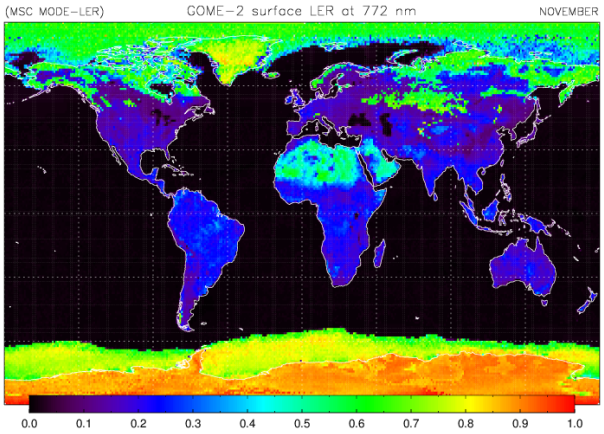

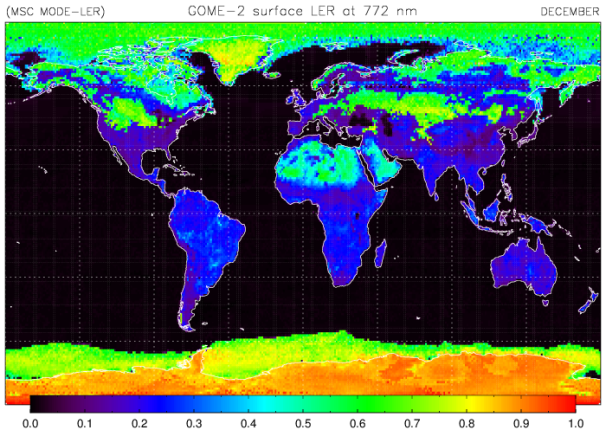

References

Burrows, J. P., et al. (1999), The Global Ozone Monitoring Experiment (GOME): Mission concept and first scientific results, *J. Atmos. Sci., 56*(2), 151–175.

EUMETSAT (2014), GOME-2 Factsheet, Doc. No. EUM/OPS/DOC/10/1299, Issue 4a, 20 May 2014, EUMETSAT, Darmstadt, Germany.

Heath, D. F., A. J. Krueger, H. A. Roeder, and B. D. Henderson (1975), The Solar Backscatter Ultraviolet and Total Ozone Mapping Spectrometer (SBUV/TOMS) for NIMBUS G, *Opt. Eng., 14*(4), 144323, doi:10.1117/12.7971839.

Herman, J. R., and E. A. Celarier (1997), Earth surface reflectivity climatology at 340–380 nm from TOMS data, *J. Geophys. Res., 102*(D23), 28,003–28,011, doi:10.1029/97JD02074.

Kleipool, Q. L., M. R. Dobber, J. F. de Haan, and P. F. Levelt (2008), Earth surface reflectance climatology from 3 years of OMI data, *J. Geophys. Res., 113*, D18308, doi:10.1029/2008JD010290.

Koelemeijer, R. B. A., J. F. de Haan, and P. Stammes (2003), A database of spectral surface reflectivity in the range 335–772 nm derived from 5.5 years of GOME observations, *J. Geophys. Res., 108*(D2), 4070, doi:10.1029/2002JD002429.

Levelt, P. F., G. H. J. van den Oord, M. R. Dobber, A. Mälkki, H. Visser, J. de Vries, P. Stammes, J.O.V. Lundell, and H. Saari (2006), The Ozone Monitoring Instrument, *IEEE Trans. Geosci. Remote Sens., 44*(5), 1093–1101, doi:10.1109/TGRS.2006.872333.

Popp, C., Wang, P., Brunner, D., Stammes, P., Zhou, Y., and Grzegorski, M. (2011), MERIS albedo climatology for FRESCO+ O2 A-band cloud retrieval, *Atmos. Meas. Tech., 4*, 463–483, doi:10.5194/amt-4-463-2011.

Tilstra, L. G., O. N. E. Tuinder, and P. Stammes (2011), GOME-2 PMD band reflectances – verification report, *KNMI Report KNMI-RP-2011-01*, Issue 2.0, Royal Netherlands Meteorological Institute, De Bilt, The Netherlands.